Title

Identification of CDKN2A Deletion as a Driver of Glioblastoma Lipid Composition and Sensitivity to Ferroptosis

Author

Morrow, Danielle

Publication Date

2021

Peer reviewed|Thesis/dissertation

UNIVERSITY OF CALIFORNIA

Los Angeles

Identification of CDKN2A Deletion as a Driver of Glioblastoma Lipid Composition and Sensitivity to Ferroptosis

A dissertation submitted in partial satisfaction of the

requirements for the degree Doctor of Philosophy

in Molecular and Medical Pharmacology

by

Danielle Harman Morrow

2021

ABSTRACT OF THE DISSERTATION

Identification of CDKN2A Deletion as a Driver of Glioblastoma Lipid Composition and Sensitivity to Ferroptosis

by

Danielle Harman Morrow

Doctor of Philosophy in Molecular and Medical Pharmacology

University of California, Los Angeles, 2021

Professor David A. Nathanson, Chair

Alterations in lipid metabolism are a hallmark of cancer and provide potential for therapeutic exploitation in the universally lethal brain tumor glioblastoma (GBM). However, an understanding of how distinct molecular features impact lipid metabolism is required for the development of effective targeted therapies. Importantly, extrinsic factors within the tumor microenvironment shape lipid metabolism, necessitating investigation within physiologic contexts. In these studies, we have performed a comprehensive characterization of the GBM lipidome through the unbiased analysis of transcriptomic, genomic, and lipidomic datasets spanning diverse tumor microenvironments and encompassing the intertumoral molecular heterogeneity observed in GBM. In the first portion of this work, we discuss the many tumor intrinsic and extrinsic factors that lead to metabolic vulnerabilities in GBM. In the second portion of this work, we identify a

novel regulator of the GBM lipidome and demonstrate the resulting metabolic vulnerabilities that occur as a result of this altered lipid metabolism.

The dissertation of Danielle Harman Morrow is approved.

Robert Prins

Steven J. Bensinger

Ajit Divakaruni

Ye Zhang

David A. Nathanson, Committee Chair

University of California, Los Angeles

2021

DEDICATION

I would like to dedicate this work to my family and friends who have supported me always.

I would also like to dedicate this work to the GBM patients who made this research possible.

TABLE OF CONTENTS

ACKNOWLEDGEMENTS

I would like to thank Professor David Nathanson for his outstanding mentorship, endless encouragement, and patient guidance throughout my graduate studies. Dr. Nathanson has been a truly excellent and dedicated mentor who always lead by example to create the amazing opportunities, laboratory, and scientific community within which to perform this work. Dr. Nathanson's mentorship helped to develop my skills as an independent scientist and contributor to the field of cancer biology, and for that I am very grateful. I would also like to thank the members of my committee, Dr. Steven Bensinger, Dr. Ajit Divakaruni, Dr. Robert Prins, and Dr. Ye Zhang, for their contributions, guidance and scientific discussions throughout my studies.

I would like to thank all of the current and past members of the Nathanson Lab for their continuous support, friendship, and encouragement throughout my time in the lab. Lisa Ta, Laura Gosa, Lynn Baufeld, Jennifer Salinas, Christopher Tse, Andrew Tum, Eva Zhou, and Rhea Plawat all contributed immensely to my studies through their involvement with tumor sample procurement, model development, and in vivo studies. Wilson Mai, Jonathan Tsang, Elizabeth Fernandez, Nicholas Bayley, Quincy Okobi, Henan Zhu, Robert Chong, and Jenna Minami provided support and scientific feedback as fellow graduate students and post-doctoral researchers. I especially would like to thank Jenna Minami for her collaboration and continuous support that made this work possible.

I would like to acknowledge my past mentors Dr. Leslie Morrow and Dr. Steve Moss for guiding me in the early stages of my research. I would not be here today were it not for those learning opportunities.

Finally, I would like to thank my family and friends. I would like to thank my parents John and Kate Morrow, my brother Alex Morrow and sister Jillian Morrow for their continuous support, love and encouragement. I would like to thank my friends who have been an incredible source of joy and strength. Finally, I want to thank my partner Kamal Singhrao for his unending support since the beginning of my time at UCLA, I am so grateful to have shared this experience with you.

Chapter 1 is a version of Morrow, D., Minami, J., Nathanson, DA. Metabolic Vulnerabilities in Brain Cancer. Neurosurg Clin N Am. 2021 Apr;32(2):159-169. doi: 10.1016/j.nec.2020.12.006. PMID: 33781499. Chapter 2 is a version of Morrow, D., Minami, J., Bayley, N., Tse, C., Salinas, J., Zhu, H., Plawat, R., Jones, A., Liau, L., Williams, K., Cloughesy, T., Dixon, S., Bensinger, S., and Nathanson, DA. CDKN2A Deletion Reprograms Lipid Metabolism Priming Glioblastoma for Ferroptosis. *In Preparation*.

My research was supported by the Department of Defense Horizon Award.

VITA

EDUCATION

2016-2021 Ph.D. Candidate, Molecular and Medical Pharmacology
University of California, Los Angeles
Department of Molecular and Medical Pharmacology
Los Angeles, CA

2008-2012 B. S., Ecology & Environmental Science
University of Maine, Orono
Orono, Maine

EMPLOYMENT

2013-2016 Research Assistant
Tufts University, Sackler School of Biomedical Science. Boston, MA

2012-2013 Research Assistant
University of North Carolina. Chapel Hill, NC

2011-2012 Undergraduate Research Assistant
University of Maine. Orono, ME

AWARDS AND HONORS

2019-2021 Peer Reviewed Cancer Research Program Horizon Award from the Department of Defense office of the Congressionally Directed Medical Research Programs

2019 UCLA CTSI Core Grant

2019 Molecular and Medical Pharmacology Retreat Poster Award

PUBLICATIONS

Morrow D, Minami J, Nathanson DA. Metabolic Vulnerabilities in Brain Cancer. Neurosurg Clin N Am. 2021 Apr;32(2):159-169. doi: 10.1016/j.nec.2020.12.006. PMID: 33781499.

Nakamura Y, **Morrow DH**, Nathanson AJ, Henley JM, Wilkinson KA, Moss SJ. Phosphorylation on Ser-359 of the α2 subunit in GABA type A receptors down-regulates their density at inhibitory synapses. J Biol Chem. 2020 Aug 28;295(35):12330-12342. doi: 10.1074/jbc.RA120.014303. Epub 2020 Jul 3. PMID: 32620552; PMCID: PMC7458806.

Nakamura Y, **Morrow D.H**, Modgil A, et al. Proteomic Characterization of Inhibitory Synapses Using a Novel pHluorin-tagged γ-Aminobutyric Acid Receptor, Type A (GABAA), α2 Subunit Knock-in Mouse. The Journal of Biological Chemistry. 2016;291(23):12394-12407. doi:10.1074/jbc.M116.724443.

Sivakumaran S, Cardarelli RA, Maguire J, Kelley MR, Silayeva L, **Morrow DH**, Mukherjee J, Moore YE, Mather RJ, Duggan ME, Brandon NJ, Dunlop J, Zicha S, Moss SJ, Deeb TZ. Selective Inhibition of KCC2 Leads to Hyperexcitability and Epileptiform Discharges in Hippocampal Slices and In Vivo. The Journal of Neuroscience. 2015;35(21):8291-8296. doi:10.1523/JNEUROSCI.5205-14.2015.

Cardarelli, R.A., Jones, K., McWilliams, L., Sharpe, P., Burnham, M., Pisella, L., Guyot, J., Dekker, N., Wobst, H., Silayeva, L., **Morrow, D.H**., Mather, R.J., Zicha, S., Davies, P., Duggan, M., Medina, I., Dunlop, J., Brandon, N., Moss, S.J. The small molecule CLP257 potentiates GABAA receptor activity but has no target engagement or functional activity at KCC2. In submission Nature Medicine

Maldonado-Devincci, A.M., Kampov-Polevoi, A., McKinley, R.E., **Morrow, D.H**., O'Buckley, T.K., Morrow, A.L. Chronic intermittent ethanol exposure alters stress effects on (3α,5α)-3-hydroxy-pregnan-20-one (3α,5α-THP) immunolabeling of amygdala neurons in C57BL/6J mice. In submission Frontiers in Cellular Science

Sivakumaran, S., Cardarelli, R.A., Maguire, J., Kelley, M.R., Silayeva, L., **Morrow, D.H**, Brandon, N.J., Dunlop, J., Zicha, S., Moss, S.J., Deeb, T.Z. Selective inhibition of KCC2 leads to hyperexcitability and unremitting epileptiform discharges in hippocampal slices. The Journal of Neuroscience 35(21): 2015 May

Cook, J.B., Nelli, S.M., Neighbors, M.R., **Morrow, D.H**., O'Buckley, T.K., Maldonado-Devincci, A.M., and Morrow, A.L. Ethanol alters local cellular levels of (3a,5a)-3-hydroxypregnan-20-one (3a,5a-THP) independent of adrenals in subcortical brain regions. Neuropsychopharmacology. 39(8):1978-87 2014 July.

Maldonado-Devincci, A.M., Cook, J.B., O'Buckley, T.K., **Morrow, D.H**., McKinley, R.E., and Morrow, A.L. Chronic Intermittent Ethanol Exposure and Withdrawal Alters (3α,5α)-3-Hydroxy-Pregnan-20-One Immunostaining in Cortical and Limbic Brain Regions of C57BL/6J Mice. Alcoholism: Clinical & Experimental Research. 38(10):2561-71 2014 Oct.

Maldonado-Devincci, A.M., Beattie MC, **Morrow, D.H**., McKinley, R.E., Cook, J.B., O'Buckley, T.K., and Morrow, A.L. Reduction of circulating and selective limbic brain levels of (3α,5α)-3-hydroxy-pregnan-20-one (3α,5α-THP) following forced swim stress in C57BL/6J mice. Psychopharmacology (Berl) 231(17):3281-92 2014 Sept.

CHAPTER 1: Metabolic Vulnerabilities in Brain Cancer

ABSTRACT

Targeting the metabolic differences between tumor and normal tissue has become a promising and novel anti-cancer therapy. Glioblastoma (GBM) exhibits altered metabolism to support a variety of bioenergetic and biosynthetic demands for tumor growth, invasion, and drug resistance. Changes in multiple metabolic pathways have been observed to help fuel tumorigenesis. Evidence in GBM and other cancers have identified that both intrinsic and extrinsic factors can impact this metabolic remodeling. Augmented oncogenic signaling due to genetic mutations and complex interactions with the tumor microenvironment (TME) impact cancer cell metabolism by changing nutrient preference, utilization, and availability. Therefore, a comprehensive understanding of GBM metabolism is critical for identifying more effective targets and therapeutics for GBM.

INTRODUCTION

Rewired cellular metabolism is a hallmark of cancer. Like most malignancies, GBMs exhibit altered metabolism to support a variety of bioenergetic and biosynthetic demands for tumor growth, invasion, and drug resistance [1,2,3]. Changes in glycolytic flux, oxidative phosphorylation, the pentose phosphate pathway, fatty acid biosynthesis and oxidation, and nucleic acid biosynthesis are observed in GBM to help drive tumorigenesis. While the mechanistic underpinnings of metabolic rewiring in GBM are still being elucidated, evidence in GBM and other cancers supports that augmented oncogenic signaling – emanating from mutations in oncogenic divers and/or loss of tumor suppressors – can rewire cellular metabolism. In addition to tumor-intrinsic drivers of metabolism, the tumor microenvironment (TME) can also impact

cancer cell metabolism via changes in nutrient availability and/or interactions with non-tumor cells. This may be particularly relevant for GBM tumors, which exist within a complex milieu of normal brain and immune cells, as well as the tightly regulated metabolic environment due to the presence of the blood brain barrier. Thus, an understanding of how both intrinsic and extrinsic factors modulate metabolism is becoming increasingly important for identifying more effective targets and therapeutics for GBM. In this review, we will outline the dynamic nature of GBM metabolism, and highlight how both molecular alterations and as well as the TME regulate metabolic remodeling in GBM (Figure 1). We will also discuss the challenges of studying metabolic interactions in the TME, and how the TME can act as a double-edged sword when considering potential therapies for GBM.

DISCUSSION

The Influence of Nature and Nurture on Metabolism in GBM

A defining feature of many cancers including GBM is increased aerobic glycolysis [4]. Despite being a less efficient source of ATP relative to oxidative phosphorylation, glycolysis enables rapid production of metabolic intermediates for macromolecular biosynthesis and improving the capacity to reduce damaging reactive oxygen species [4]. Notably, GBM cells display a dependency on glycolysis for growth and survival [5,6]. The enhanced glycolytic phenotype observed in GBM tumors is, at least in part, driven by various recurring oncogenic mutations. For example, a defining feature of GBM is the upregulation and constitutive activation of the receptor tyrosine kinase epidermal growth factor receptor (EGFR), which is highly correlated with decreased patient prognosis and occurs in approximately 60% of GBM tumors [3]. The most frequent

activating mutation in EGFR found in GBM – a ligand independent variant termed EGFRvIII – can drive glycolysis via c-MYC activation, which can drive glycolytic gene expression, specifically increasing the expression of Glucose Transporters 1 (GLUT1) and 3 (GLUT3), Hexokinase2 (HK2), and Pyruvate Dehydrogenase Kinase (PDK1) [7,8]. Moreover, hyperactivated EGFR signaling in GBM can also promote heightened glucose metabolism via regulating the plasma membrane localization of GLUT1 and GLUT3 [3]. Notably, targeting EGFR-driven glucose metabolism can consequently engage the intrinsic apoptotic machinery in primary GBM cells [3], emphasizing the importance of this relationship for GBM growth and viability.

Mutations in the tumor suppressor, TP53, are another common feature of GBM tumors [9]. Although not directly shown in GBM, loss of function mutations in TP53 can increase aerobic glycolysis via altered regulation of the glucose transporter genes GLUT1 and GLUT4 [7]. Critically, cytoplasmic p53 in GBM has been shown to connect EGFR-driven glucose metabolism to apoptosis, indicating dependencies in the crosstalk between oncogenic signaling and metabolism [3]. However, heightened glycolysis is not universal to all GBM. A defining feature of low-grade glioblastomas, isocitrate dehydrogenase 1 (IDH1) mutations inhibit glucose uptake by reducing expression of lactate dehydrogenase A (LDHA) which converts glucose to lactate. As a result, mutations in IDH1 in GBM gliomaspheres were shown to result in reduced glucose uptake compared to IDH wild type gliomaspheres, as well as reduced uptake of the glucose analog fluorodeoxyglucose (FDG) *in vivo* [10,11].

Many cancers upregulate flux through the pentose phosphate pathway (PPP) to drive the synthesis of nucleotides for DNA replication and repair, as well as the production of reducing equivalents (e.g., NADPH) to support redox homeostasis and lipid biosynthesis [12]. Entry into the

PPP proceeds via the conversion of glucose-6 phosphate by Glucose-6-phosphate dehydrogenase into 6-phosphogluconolactone and, via additional enzymatic steps, ultimately producing ribulose-5-phosphate, CO2, and NADPH [12]. Through the oxidative branch of this pathway, glucose is converted to NADPH and ribonucleotides [12]. Nucleotide biosynthesis is critical to support rapidly proliferating cells, and de novo biosynthesis of both purines and pyrimidines has been observed to be altered in cancers [12]. A recent study found that low levels of nucleobase containing metabolites were strongly associated with sensitivity to radiation therapy [13] in GBM, and that supplementing GBM cells with exogenous nucleotides protected them from radiation by promoting repair of double-stranded breaks. The protective effects of these nucleotides were found to be due to purines, as de novo purine biosynthesis can generate GTP, which thus promotes tRNA and rRNA synthesis [14]. Together, these findings suggest that modulating purine biosynthesis through targeting the non-oxidative branch of the PPP may radiosensitize GBM. It has also been shown in GBM that the rate-limiting enzyme for de novo guanine nucleotide biosynthesis, IMP dehydrogenase (IMPDH2), is upregulated and results in increased de novo GTP biosynthesis [15]. Contrary to normal primary glial cells which can utilize the salvage pathway, inhibition of IMPDH2 in glioblastoma cells reduced nucleotide synthesis and proliferation [15]. Finally, the combination of targeting both de novo and salvage pyrmidine biosynthesis can significantly impair primary GBM cell growth and survival [16].

In many cancers, oxidative phosphorylation (OXPHOS) is upregulated even in the presence of increased glycolysis [17]. OXPHOS produces ATP via the transfer of electrons from NADH or $FADH_2$ to oxygen via electron carriers in the inner mitochondrial membrane, known as the electron transport chain. This process produces a proton gradient that enables ATP synthesis via phosphorylation of ADP [17]. There are multiple pro-tumorigenic consequences of increased

OXPHOS, including the production of reactive oxygen species (ROS) which can increase proliferation, survival signaling, and genomic instability [18]. Additionally, the ability of tumor cells to utilize both glycolysis and oxidative phosphorylation confers metabolic flexibility that may contribute to therapeutic resistance [19]. Importantly, the ability of cells to utilize OXPHOS may be impacted not only by respiratory capacity, but also by oxygen availability within the tumor microenvironment [20]. In vivo analysis of GBM tumor metabolism via isotopically labeled nutrient infusion identified that molecularly diverse GBM utilize both glycolysis and mitochondrial glucose oxidation [21]. Importantly, multiple studies have demonstrated that OXPHOS represents a targetable vulnerability in GBM cells. For example, IMP2 was shown to be both highly expressed and a critical regulator of OXPHOS in GBM. Consequently, ablation of IMP2 or treatment with the Complex I inhibitor rotenone could inhibit GBM cell growth [22]. Moreover, a recent study demonstrated that the ATP synthase inhibitor, Gboxin, could reduce *in vitro* and *in vivo* proliferation of primary GBM cells, presumably as a consequence of impaired energy production [23].

Cancers can utilize multiple bioenergetic substrates for OXPHOS, including fatty acids, ketone bodies, glutamate, and acetate [24]. The ability to alternate between these substrates based on nutrient availability may provide these tumors with a metabolic advantage. Studies conducted by Mashimo and Pichumani et al revealed that, in GBM patient-derived xenograft (PDX) models, acetate, a widely available nutrient in the brain, served as a critical bioenergetic substrate in the microenvironment for human GBM [25]. Six GBM PDX models received infusions of 13C-labelled acetate and glucose, and 13C-nuclear magnetic resonance (NMR) analysis revealed that GBMs exhibited a shift towards acetate oxidation to acetyl-CoA. They also found that levels of acetyl-CoA synthetase 2 (ACCS2), an enzyme that converts acetate to acetyl-CoA, was high in GBM

PDX tumors, and that ACSS2 expression was inversely correlated with GBM patient survival [25]. Astrocytes have the capability to utilize acetate under limited glucose conditions, including diabetic hypoglycemia [26]. Therefore, the capacity to metabolize acetate may result from the astro-glial lineage of GBM [25]. Further research is needed to elucidate the role of molecular heterogeneity and tumor microenvironment on oxidative capacity.

Glutamine serves as a source of nitrogen and carbon for the biosynthesis of nucleotides and amino acids, as well as a potential fuel source for the TCA [27]. In normal brain tissue, glutamate can be taken up by astrocytes via astrocytic glutamate transporters and subsequently synthesized to glutamine [28,29]. Glutamine is then transported to neurons, where it is converted back to glutamate for synaptic transmission through a process that is termed the glutamine-glutamate cycle [30,31]. The glutamine/glutamate rich brain microenvironment enables brain tumors to make synaptic connections with glutamatergic neurons and reprogram glutamine metabolism to enable growth [32,33,34]. Indeed, glutamine metabolism was found to be increased in human GBM xenografts compared to surrounding brain tissue [21]. Under glutamine-starved conditions, GBM cells can either convert glutamate into glutamine via upregulation of glutamine synthetase (GS) or uptake astrocyte-derived glutamine via ASCT2 [35]. *In vivo* isotope-tracing studies have identified that human GBM cell lines and patient-derived xenografts preferentially utilize glucose over glutamine to supply TCA cycle intermediates [21,25], with glucose-derived carbons supporting glutamine synthesis from glutamate [35,36]. The findings from these studies suggest that GBMs do not utilize glutamine as a major fuel for the TCA cycle; however, other studies conducted *in vitro* have suggested that primary glioma cell lines do require glutamine to support oxidative metabolism [37]. The discrepancy between these findings highlights the differences between the in vitro and in vivo

microenvironment and raises the question of whether in vitro nutrient dependencies are metabolic adaptations to the non-physiologically relevant nutrient concentration in media [38,39].

The role of glutamine in GBM has also been shown to be dictated by the presence of genetic alterations in glutamine metabolism. IDH1 and IDH2 mutations catalyze the production of the oncometabolite D-2-hydroxyglutarate (D2HG) from alpha-ketoglutarate [40]. D2HG inhibits DNA and histone demethylases, resulting in the inhibition of cell differentiation. In vivo studies of patient-derived chondrosarcoma IDH1 mutant xenografts revealed that glutamine is a primary carbon source for D2HG [41]. However, the role of D2HG has yet to be fully elucidated in the brain tumor microenvironment, and recent studies point to interactions between D2HG and the immune cell milleu of the tumor microenvironment [42]. In vivo syngeneic mouse models of IDH1 mutant glioblastoma have shown that D2HG decreases CXCL10 expression, resulting in a reduction of T cell accumulation at the tumor site [43]. Further in vivo studies are required to understand the extent to which production of this oncometabolite may lead to immune cell evasion and cancer progression.

Rapidly proliferating tumor cells require increased biosynthesis and uptake of fatty acids to form new cellular membranes during cell division, support increased post-translation modification of signaling molecules, and serve as energy stores [39]. The brain is a distinctly unique microenvironment when it comes to lipid metabolism. Lipid molecules are key components of the brain's structure and comprise around 50% of the brain's dry weight [44,45]. Several recent studies have provided evidence that fatty acids, including essential fatty acids obtained from the diet, can cross the blood-brain barrier (BBB) and be taken up by neurons via fatty acid transporters [45]. Unlike fatty acids, all cholesterol obtained in the CNS must be formed in situ, as the brain cannot

access dietary or hepatic cholesterol due to the BBB [46,47]. While both neurons and astrocytes can make cholesterol de novo, the major input of cholesterol into the brain originates from in situ synthesis in the endoplasmic reticulum (ER) of astrocytes [48]. Neurons and astrocytes both produce oxysterols as a product of cholesterol metabolism, which acts as an endogenous ligand for liver X receptors (LXRs). LXR activation decreases excess cellular cholesterol and by promoting efflux through sterol transporters [49], maintaining cholesterol homeostasis within the brain. Previous studies have shown that GBM cells display dysregulated cholesterol metabolism and accumulate astrocyte-derived cholesterol from the brain microenvironment [50]. GBM cells were also found to suppress LXR ligand synthesis – treatment of GBM with LXR agonists killed GBM cell lines in vitro, while sparing normal human astrocytes (NHAs) [50].

GBM cells also contain higher levels of cholesterol esters (CEs) and triacylglycerides (TAGs) than normal surrounding brain tissue [51]. Several studies have documented an increased number of lipid droplets in GBM cells, which are composed of CEs and TAGs, as a characteristic feature of GBM tumor cells in vivo [52]. Recently, it was shown that monounsaturated fatty acids increase lipid droplet formation and fatty acid oxidation in GBM, which was also associated with increased rates of glycolysis and cell proliferation [53]. Interestingly, a key characteristic of astrocytes is the formation of lipid droplets, which act as a buffer for neurons experiencing high stress. Studies have shown that stressed neurons induce astrocyte lipid droplet formation by shuttling their oxidized fatty acids to neighboring astrocytes [54] –the ability for GBMs to synthesize lipid droplets may again hint to their astro-glial lineage, yet future studies are necessary to connect cell of origin to metabolic phenotype.

Several genetic alterations common the GBM have been implicated in lipid metabolic reprograming in cancer. It has been shown that EGFR activates the transcription factor SREBP-1, a master regulator of lipid metabolism [55]. Consequently, inhibition of fatty acid synthesis rendered EGFRvIII, and not EGFR wild type GBM, sensitive to cell death, indicating an EGFRvIII-dependent lipid metabolic vulnerability [55]. In breast cancer cells, mutant P53 was shown to bind to and activate SREBPs, leading to enhancement of the mevalonate pathway to upregulate cholesterol biosynthesis and increase proliferation [56]. EGFRvIII signaling has been shown to induce phospholipid remodeling via LPCAT1 by saturating phosphatidylcholine lipid species. Interestingly, the LPCAT1-mediated shift towards saturated phospholipids also regulates EGFRvIII signaling by controlling the amount of EGFRvIII on the plasma membrane [54] and targeting LPCAT1 caused EGFRvIII to dissociate from cellular membranes, inducing massive tumor death [54]. Aberrant phospholipid metabolism was also identified via in situ MALDI imaging of patient-derived orthotopic IDH1 mutant GBM xenografts compared to IDH1wt tumors [57]. Comprehensive metabolic profiling comparing low grade astrocytoma (LGA) and GBM patient-derived tumors revealed a shift from fatty acid synthesis to catabolism in GBM, with fatty acid beta-oxidation (FAO) being a key node differentiating GBM from LGA [58]. FAO can serve both cataplerotic and cataplerotic roles, and is thought to provide metabolic plasticity in GBM, allowing these cells to accommodate to its harsh microenvironment.

Numerous microenvironmental factors may impact tumor metabolism. Indeed, it has been hypothesized that the tumor microenvironment dictates inter-tumoral metabolic heterogeneity [59]. A consequence of overwhelming the vascular supply in the brain, hypoxia has been shown to correlate with tumor aggressiveness and poor patient prognosis [60, 61]. HIF transcription factors are regulators of the adaptive response to hypoxia that are frequently upregulated in GBM [62]. The

transcription factor HIF-1α is activated during hypoxia, leading to the activation of enzymes that stimulate glycolytic flux to lactate efflux into the extracellular matrix [63]. Export of lactate acidifies the tumor environment, which can induce local pro-tumorigenic inflammatory responses [63] and enhance tumor cell invasion [62], further highlighting the interactions between GBM and the tumor microenvironment. Finally, stabilization of HIF-1a could also lead to decreased cell proliferation [64]. Whilst counterintuitive, a hypoxic TME could result in a problematic population of cells that can survive under hypoxic stress and overcome common cancer therapeutics. Given that most cancer drugs are designed to target rapidly proliferating cells, tumor cells in a hypoxic niche may evade these therapeutics by demonstrating decreased proliferation. Low oxygen tension also results in an acidic environment, which can inhibit drug uptake rates via diffusion due to polarization of the cell membrane [65]. However, this key factor may be lost or overlooked in cell culture, as cells are often cultured under normoxic conditions [66]. In vitro studies have shown that hypoxia alters the GBM metabolome by transcriptional regulation of key metabolic enzymes [67]. Among the observed alterations are increased glycolysis and biosynthesis of macromolecules and nucleotide cofactor NAD and NADP biosynthesis, as well as the oncometabolite 2-hydroxyglutarate [67]. Additionally, hypoxia induces a decrease in TCA cycle intermediates and altered cholesterol, glycerolipid, and sphingolipid metabolism. Engel et al recently demonstrated that modulating serine availability under conditions mirroring the GBM microenvironment sensitized GBM cells to hypoxia-induced cell death by increased ROS [64].

TME Influence on GBM Metabolism: Implications for Experimental and Translational Studies

The unique features of the brain TME pose a difficult challenge when studying GBM and other primary brain cancers. The brain consumes 25% of the body's glucose, 20% of its oxygen, and is comprised largely of lipids [45,68]. Moreover, recent evidence supports that cancer cells, including GBM, can shift their metabolic flux in response to nutrient availability in the tumor microenvironment (TME) [58,69]. While the impact of physical environmental factors on cell metabolism is beginning to be appreciated [70,71], an understanding of nutrient availability within the GBM TME remains largely understudied.

Although advances in methodologies have provided researchers much insight into cancer biology, deploying these experiments in the appropriate model system remains crucial. Investigations of TME-tumor metabolic interactions remain sparse due to the lack of model systems that appropriately recapitulate the brain microenvironment. There are often trade-offs between the physiological-relevance of a given model and its tractability for experiments – orthotopic xenograft models can recapitulate GBM progression in the brain; however, these models are inherently complex and most-likely lack an immune system. In contrast, in vitro culture models are experimentally tractable, but rely on studying cells in a context that is vastly different metabolic environment from that of the TME.

The presence of intratumoral heterogeneity renders in vitro modeling of GBM exceptionally challenging when studying metabolism [72,73,74]. Additionally, cell culture media does not accurately recapitulate nutrient levels within the TME [39]. Classical synthetic cell culture media contains glucose, amino acids, vitamins, and salts that largely do not reflect those of human plasma

or cerebral spinal fluid (CSF), and lack additional components such as lipids and nucleotide precursors [75,76]. Investigations into the effect of DMEM/F12 media on neuronal activity found that the supraphysiological levels of calcium (2-3 times higher than brain concentrations) impaired synaptic activity and reduced synaptic communication and action potential firing [77]. Disruptions to glucose homeostasis is known to disrupt brain physiology, and levels of glucose in DMEM and Neurobasal media are roughly 2-5 times higher than glucose levels in the brain of hyperglycemic patients [78]. 3D organoids grown from GBM cells and biopsies have become an increasingly popular method for modeling GBM in vitro – while organoid culture maintains regional heterogeneity and tissue architecture of the brain TME, it still lacks physiological nutrient levels as the media used for organoid culture may not be representative of the nutrient milieu found in tumors in vivo [79]. In vitro models may also select against tumors that are auxotrophic for particular nutrients found in the TME but not found in cell culture media [76,80], potentially leaving these tumors underrepresented and understudied. While in vivo models may better represent the complexity and heterogeneity of cells within the brain tumor microenvironment, when using mouse models to study metabolism, multiple factors such as strain, diet, sex, age, and environment stressors should be considered, as these could affect tumor metabolism [80,81].

Both biochemical and genetic experiments support the notion that the TME impacts metabolism. As mentioned above, stable-isotope tracing experiments have shown that tricarboxylic acid (TCA) cycle substrates can be utilized differently between in vivo and in vitro conditions. For example, Davidson et al showed that in two-dimensional culture models of lung cancer, glutamine is the primary carbon substrate for the TCA cycle; however, experiments performed in lung tumors in vivo suggest that tumors favor the use of glucose for TCA cycle intermediates [38, 82]. Similarly, GBM cells in culture appear to be dependent on glutamine for TCA

cycle anapleurosis [35]; however, experiments performed in vivo suggest that GBM tumors utilize other TCA cycle substrates and are even glutamine autonomous [35]. Moreover, cancer cells in human plasma-like media drastically altered the metabolism of cells compared to that in traditional media and inhibited de novo pyrimidine synthesis [75]. At concentrations present in human plasma, uric acid, a metabolite not found in traditional cell culture media, was found to be an endogenous inhibitor of uridine monophosphate synthase (UMPS), which catalyzes the last two steps in de novo pyrimidine synthesis [75]. Finally, recent genetic experiments have identified vast differences in metabolic pathway utilization between in vitro culture models and in vivo tumor models – RNAi and CRISPR screens performed to identify essential metabolic enzymes share little overlap in the essential enzymes these screens identified between model systems [83,84]. Collectively, these studies highlight how model environment can shape specific nutrient consumption and utilization; which, may have profound implications on assessment of a metabolic dependency of a tumor.

Therapeutic Opportunities: Unraveling metabolic dependencies in GBM

Metabolic reprogramming arises as a consequence of interactions between the altered intrinsic characteristics of the tumor and the unique tissue context that fuels aggressive proliferation. Metabolic interactions between the tumor and microenvironment present a double-edged sword and can both fuel and hinder GBM. Nutrients obtained from the microenvironment can regulate signaling pathways through nutrient sensors, such as mTORC1 and AMPK, which support the metabolic demands of the tumor [85]. Cancer cells can also compete with infiltrating immune cells for nutrients that are limited in the TME, and secretion of metabolic byproducts can create an immunosuppressive niche that limits antitumor immune responses [86]. Likewise,

interactions between oncogenic alterations and the microenvironment can select for favorable metabolic dependencies, which can present a therapeutic opportunity. EGFR presents a promising molecularly targeted metabolic therapy. In their paper, Mai et al discovered a subset of GBMs termed "metabolic responders" that exhibit EGFR-driven glucose utilization. ^{18}F-FDG PET scans revealed that GBMs classified as metabolic responders had decreased glucose metabolism after EGFR-inhibition; importantly, while EGFR-inhibition alone did not cause significant cell death, it primed the cells for apoptosis [3], creating an opportunity for synthetic lethality. Molecular therapies targeting mutant IDH has also become an attractive and promising therapeutic strategy, as it reduces the tumorigenic properties of D2HG. Phase I studies of two mutant IDH1 inhibitors (AGI-881, AG-120) showed favorable safety and efficacy in patients with IDH mutated gliomas [22], and ivosidenib (AG-120) has been approved by the Food and Drug Administration (FDA) as a first-line treatment for IDH1-mutant acute myeloid leukemia (AML) [42]. Several lines of evidence also suggest that indirect targeting of mutant IDH through its metabolic vulnerabilities could also prove beneficial. Patients with IDH mutant GBMs seem to have a better prognosis than those with IDH wild type GBM; however, it is not clear whether this is due to D2HG mediated vulnerabilities or the histology between these two tumor types [43]. D2HG has been shown to decrease the glycolytic capacity [10,11]; therefore, targeting energy production may decrease tumor growth and proliferation in IDH mutant GBM.

Metabolic dependencies in gliomas arise as a consequence of many factors, including tumor genotype, cell line lineage, and environmental context (Figure 2). Therefore, studies that consider these factors in isolation may not identify translatable therapeutic targets [57]. Relying solely on *in vivo* models to identify metabolic targets is impractical; however, current *in vitro* models do not fully recapitulate the physiological microenvironment of tumors. Aspects of the

physical and biochemical environment can alter therapeutic response, and differences in nutrient utilization between tumor and tissue could present targetable liabilities in cancer. The ketogenic diet (KD) has been used for over 90 years as a treatment for drug-resistant seizures in children and adults with epilepsy [55]. This diet relies on fat as the main source of energy, and a drastic decrease in carbohydrate intake to induce ketosis [56] while the normal brain can utilize ketones as an alternate energy source, it has been shown that certain GBMs do not have the metabolic flexibility to do so, and glucose depletion through the KD could deprive GBMs of their main energy supply [87,88]. Despite the potential of utilizing the KD to treat GBM, the practical application of this therapy has been limited in clinical studies, as patient compliance to the KD is difficult due to severely limited carbohydrate intake [56]. In the setting of dietary therapy for GBM, clinicians specialized in nutrition should be included in the neuro-oncology team. Treatment through dietary alterations may be particularly effective for patients with highly glycolytic GBMs and could be implemented as a monotherapy or in conjunction with anti-glycolytic drugs, molecular therapies, or radiation and chemotherapies.

As previously proposed, a comprehensive analysis would require studies that integrate both *in vitro* and *in vivo* patient derived cell line models, studies in patients, and ultimately clinical trials [57]. A systems biology approach that integrates multiple data types and contextual information may yield novel vulnerabilities that are missed when examining single molecular features in isolation. Although progress has been made in deciphering the metabolic network of GBM, there is still much to be learned about how both genetic aspects in the environmental context of the brain TME determine metabolic vulnerabilities. Applying a comprehensive analysis will allow us to unravel the intricacies of the multi-faceted metabolic interactions in GBM.

FIGURES

Chapter 1 – Figure 1.

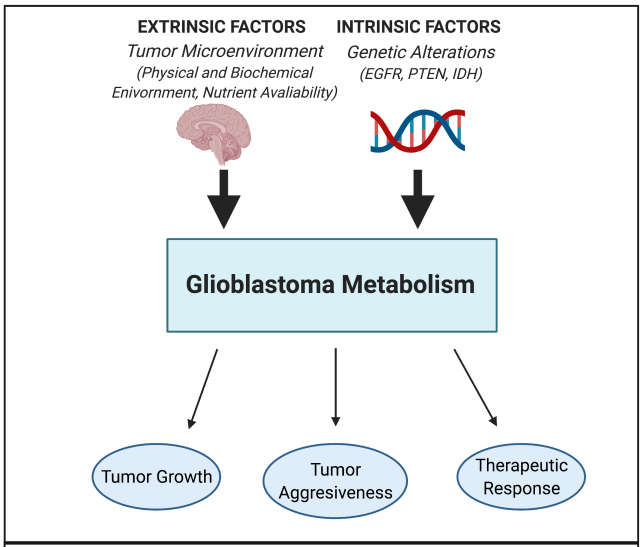

Figure 1: Glioblastoma metabolism - influential factors and outcomes

Chapter 1 – Figure 2.

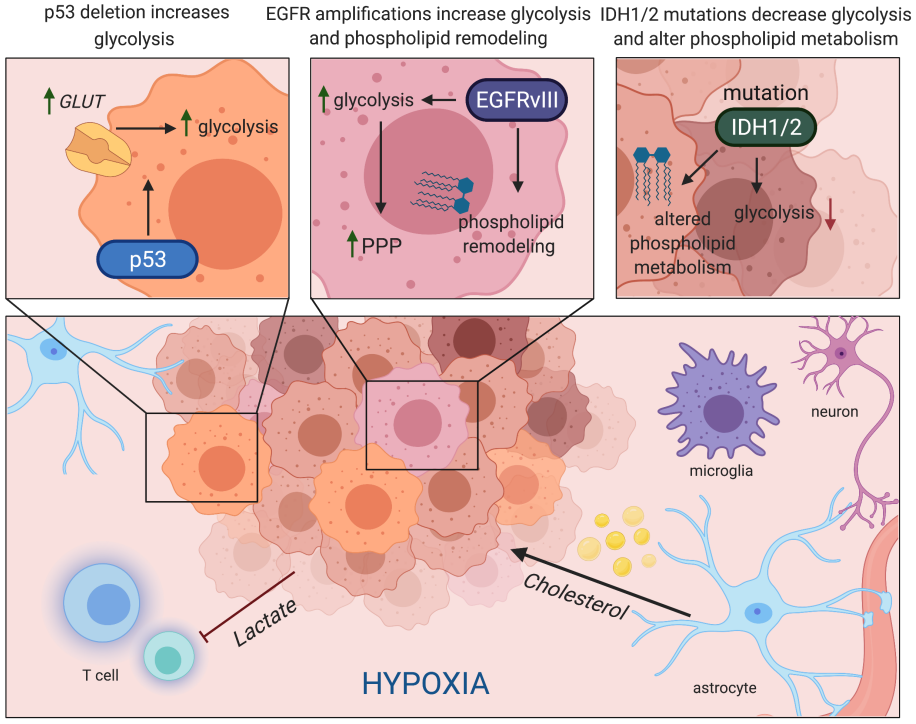

Figure 2:

Examples of metabolic remodeling in GBM. Genetic alterations rewire metabolism in GBM - EGFR amplifications and mutations can increase glycolysis and PPP activity (upper middle) furthermore, EGFRvIII has been shown to induce phospholipid remodeling. Loss of p53 increases glycolysis by activating GLUTs (upper left). IDH1/2 mutations decrease glycolysis by reducing LDH expression. 2-hydroxyglutarate (2HG), the metabolic byproduct produced by mutant IDH1/2, also can alter epigenetic modifications (upper right). Finally, GBM metabolism is both rewired by and can rewire the TME. GBMs can uptake astrocyte-derived cholesterol to meet increased metabolic demands and can release lactate into the environment to suppress immune cells. The acidic and hypoxic TME also can promote aerobic glycolysis, tumor invasion, and resistance to certain therapeutics (bottom).

REFERENCES

1. Venneti S and Thompson CB (2017). Metabolic programming in brain tumors. Annual Review of Pathology: Mechanisms of Disease, 12(1):515-545.

2. Pavlova, N. N., & Thompson, C. B. (2016). The emerging hallmarks of cancer metabolism. Cell Metabolism, 23(1), 27–47.

3. Mai, W. et. al. (2017) Cytoplasmic p53 couples oncogene-driven glucose metabolism to apoptosis and is a therapeutic target in glioblastoma. Nature Medicine. 23(11): 1342-1351.

4. Vander Heiden MG, Cantley LC, Thompson CB (2009). Understanding the Warburg effect: the metabolic requirements of cell proliferation. Science. 324(5930):1029-33.

5. Amparo Wolf, Sameer Agnihotri, Johann Micallef, Joydeep Mukherjee, Nesrin Sabha, Rob Cairns, Cynthia Hawkins, Abhijit Guha; Hexokinase 2 is a key mediator of aerobic glycolysis and promotes tumor growth in human glioblastoma multiforme. J Exp Med 14 February 2011; 208 (2): 313–326. doi: https://doi.org/10.1084/jem.20101470

6. Flavahan, W. A., Wu, Q., Hitomi, M., Rahim, N., Kim, Y., Sloan, A. E., Weil, R. J., Nakano, I., Sarkaria, J. N., Stringer, B. W., Day, B. W., Li, M., Lathia, J. D., Rich, J. N., & Hjelmeland, A. B. (2013). Brain tumor initiating cells adapt to restricted nutrition through preferential glucose uptake. Nature neuroscience, 16(10), 1373–1382. https://doi.org/10.1038/nn.3510

7. Babic, I., Anderson, E. S., Tanaka, K., Guo, D., Masui, K., Li, B., Zhu, S., Gu, Y., Villa, G. R., Akhavan, D., Nathanson, D., Gini, B., Mareninov, S., Li, R., Camacho, C. E., Kurdistani, S. K., Eskin, A., Nelson, S. F., Yong, W. H., Cavenee, W. K., … Mischel, P. S. (2013). EGFR mutation-induced alternative splicing of Max contributes to growth of glycolytic tumors in brain cancer. Cell metabolism, 17(6), 1000–1008.

8. Levine AJ and Puzio-Kutre AM (2010). The control of the metabolic switch in cancers by oncogenes and tumor suppressor genes. Science, 330*6009):1340-1344.

9. Brennan, C. W., Verhaak, R. G., McKenna, A., Campos, B., Noushmehr, H., Salama, S. R., Zheng, S., Chakravarty, D., Sanborn, J. Z., Berman, S. H., Beroukhim, R., Bernard, B., Wu, C. J., Genovese, G., Shmulevich, I., Barnholtz-Sloan, J., Zou, L., Vegesna, R., Shukla, S. A., Ciriello, G., … TCGA Research Network (2013). The somatic genomic landscape of glioblastoma. Cell, 155(2), 462–477. https://doi.org/10.1016/j.cell.2013.09.034

10. Garrett, M., Sperry, J., Braas, D., Yan, W., Le, T. M., Mottahedeh, J., Ludwig, K., Eskin, A., Qin, Y., Levy, R., Breunig, J. J., Pajonk, F., Graeber, T. G., Radu, C. G., Christofk, H., Prins, R. M., Lai, A., Liau, L. M., Coppola, G., & Kornblum, H. I. (2018). Metabolic

characterization of isocitrate dehydrogenase (IDH) mutant and IDH wildtype gliomaspheres uncovers cell type-specific vulnerabilities. Cancer & metabolism, 6, 4

11. Kim, D. et. al., (2017) IDH1 mutation is associated with low FDG upatke in cerebral gliomas associated with low FDG uptake in cerebral gliomas. The Journal of Nuclear Medicine. Vol 58.

12. Patra KC, Hay N (2014). The pentose phosphate pathway and cancer. Trends in Biochemical Sciences. 39(8):347-354

13. Ahmad, F., Dixit, D., Sharma, V. et al (2016). Nrf2-driven TERT regulates pentose phosphate pathway in glioblastoma. Cell Death Dis 7, e2213.

14. Zhou W, Yao Y, … Wahl D (2020). Purine metabolism regulates DNA repair and therapy resistance in glioblastoma. Nature Communications, 3811.

15. Kofuji S, et al. IMP dehydrogenase-2 drives aberrant nucleolar activity and promotes tumorigenesis in glioblastoma. Nat Cell Biol. 2019 Aug;21(8):1003-1014. doi: 10.1038/s41556-019-0363-9. Epub 2019 Aug 1. PMID: 31371825; PMCID: PMC6686884.

16. Dan R. Laks, Lisa Ta, Thomas J. Crisman, Fuying Gao, Giovanni Coppola, Caius G. Radu, David A. Nathanson and Harley I. Kornblum (2016). Inhibition of Nucleotide Synthesis Targets Brain Tumor Stem Cells in a Subset of Glioblastoma. Mol Cancer Ther June 1 2016 (15) (6) 1271-1278; DOI: 10.1158/1535-7163.MCT-15-0982

17. Ashton, T. M., McKenna, W. G., Kunz-Schughart, L. A., & Higgins G. S. (2018). Oxidative Phosphorylation as an Emerging Target in Cancer Therapy. Clinical Cancer Research.

18. Liou GY and Storz P (2010). Reactive oxygen species in cancer. Free Radical Research. 44(5).

19. McGuirk, S., Audet-Delage, Y., & St-Pierre, J. (2020) Metabolic fitness and plasticity in cancer progression. Trends in Cancer. 6(1):49-61 DOI:https://doi.org/10.1016/j.trecan.2019.11.009
20. 20.Vaupel P, Mayer A (2012). Availability, not respiratory capacity governs oxygen consumption of solid tumors. Int J Biochem Cell Biol. 44:1477–81

21. Marin-Valencia I., Yang C., Mashimo T., Cho S., Baek H., Yang X.L., Rajagopalan K.N., Maddie M., Vemireddy V., Zhao Z., et al. Analysis of tumor metabolism reveals mitochondrial glucose oxidation in genetically diverse human glioblastomas in the mouse brain in vivo. Cell Metab. 2012;15:827–837.

22. Janiszewska, M., Suvà, M. L., Riggi, N., Houtkooper, R. H., Auwerx, J., Clément-Schatlo, V., Radovanovic, I., Rheinbay, E., Provero, P., & Stamenkovic, I. (2012). Imp2

controls oxidative phosphorylation and is crucial for preserving glioblastoma cancer stem cells. Genes & development, 26(17), 1926–1944. https://doi.org/10.1101/gad.188292.112

23. Molina, J.R., Sun, Y., Protopopova, M. et al. (2018). An inhibitor of oxidative phosphorylation exploits cancer vulnerability. Nat Med 24, 1036–1046

24. Mafeezzini, C, Calvo-Garrido, J, Wredenberg, A, and Freyer, C (2020). Metabolic regulation of neurodifferentiation in the adult brain. Cellular and Molecular Life Sciences, 77: 2483-2486.

25. Mashimo T., Pichumani K., Vemireddy V., Hatanpaa K. J., Singh D. K., Sirasanagandla S., et al. . (2014). Acetate is a bioenergetic substrate for human glioblastoma and brain metastases. Cell 159, 1603–1614.

26. Jiang L, Gulanski BI, De Feyter HM, Weinzimer SA, Pittman B, Guidone E, Koretski J, Harman S, Petrakis IL, Krystal JH, Mason GF, (2013). Increased brain uptake and oxidation of acetate in heavy drinkers. J. Clin. Invest 123 (4), 1605–1614

27. DeBerardinis, R.J.; Mancuso, A.; Daikhin, E.; Nissim, I.; Yudko_, M.; Wehrli, S.; Thompson, C.B. Beyond aerobic glycolysis: Transformed cells can engage in glutamine metabolism that exceeds the requirement for protein and nucleotide synthesis. Proc. Natl. Acad. Sci. USA 2007, 104, 19345–19350.

28. Sequerra EB, Goyal R, Castro PA, Levin JB, and Borodinsky LN (2018). NMDA receptor signaling is important for neural tube formation and for preventing antiepileptic drug-induced neural tube defects. Journal of Neuroscience, 2634.

29. Hamberger A, Nystrom B, Larsson S, Silfvenius H, Nordborg, C, (1991). Amino Acids in the neuronal microenvironment of focal human epileptic lesions. Epilepsy Research, 9(1):32-43.

30. Hertz L, (2013). The glutamate-glutamine (GABA) cycle: importance of late postnatal development and potential reciprocal interactions between biosynthesis and degradation. Frontiers in Endocrinology, 4(59).

31. Daikhin Y, Yudkoff M, (2000). Compartmentation of brain glutamate metabolism in neurons and glia. J Nutr, 130(1026-1031).

32. Venkatesh, HS, Morishita W, Geraghty AC, Silverbush D, … Malenka RC, Monje M (2019). Electrical and synaptic integration of glioma into neural circuits. Nature, 573:549-545.

33. Venkataramani V, Ivanov Tanev D. Kuner T (2019). Glutamatergic synaptic input to glioma cells drives brain tumour progression. Nature, 573:532-538.

34. Sidoryk M, Matyja E, Dybel A… Albrecht J (2004). Increase expression of glutamine transporter SNAT3 is a marker of malignant gliomas. Neuroreport. 15(4):575-578.

35. Tardito, S. et al. (2015). Glutamine synthetase activity fuels nucleotide biosynthesis and supports growth of glutamine-restricted glioblastoma. Nat. Cell Biol. 17, 1556–1568.

36. Cheng, T, Sudderth J, Yang C, Mullen AR, Jin ES, Mates JM, DeBerardinis RJ (2001). Pyruvate carboxylase is required for glutamine-independent growth of tumor cells. Proc Natl Acad Sci USA, 108(21):8674-8679.

37. Oizel K, Chauvin C, Oliver L, Gratas C… Vallette FM, Pecqueur C (2017). Efficient mitochondrial glutamine targeting prevails over glioblastoma metabolic plasticity. Clinical Cancer Research, 23(20).

38. S.M. Davidson, T. Papagiannakopoulos, B.A. Olenchock, J.E. Heyman, M.A. Keibler, A. Luengo, M.R. Bauer, A.K. Jha, J.P. O'Brien, K.A. Pierce, et al (2016). Environment impacts the metabolic dependencies of Ras-driven non-small cell lung cancer. Cell Metab., 23:517-528.

39. Lagziel S, Gottlieb E, Sholomi T, (2020). Mind your media. Nature metabolism.

40. Zhou, W., & Wahl, D. R. (2019). Metabolic Abnormalities in Glioblastoma and Metabolic Strategies to Overcome Treatment Resistance. Cancers, 11(9), 1231

41. Salamanca-Cardona, L., Shah, H., Poot, A. J., Correa, F. M., Di Gialleonardo, V., Lui, H., Miloushev, V. Z., Granlund, K. L., Tee, S. S., Cross, J. R., Thompson, C. B., & Keshari, K. R. (2017). In Vivo Imaging of Glutamine Metabolism to the Oncometabolite 2-Hydroxyglutarate in IDH1/2 Mutant Tumors. Cell metabolism, 26(6), 830–841.e3.

42. Zhang L, Sorensen MD, Kristensen BW, Reifenberger G, McIntyre TM, Lin F. D-2-Hydroxyglutarate Is an Intercellular Mediator in IDH-Mutant Gliomas Inhibiting Complement and T Cells. Clin Cancer Res. 2018 Nov 1;24(21):5381-5391. doi: 10.1158/1078-0432.CCR-17-3855. Epub 2018 Jul 13. PMID: 30006485; PMCID: PMC6214730.

43. Isocitrate dehydrogenase mutations suppress STAT1 and CD8+ T cell accumulation in gliomas.

44. O'Brien JS, Sampson EL. Lipid Composition of the normal human brain: gray matter, white matter, and myelin. J Lipid Res. 6(4):537-544.

45. Bruce, K. D., Zsombok, A. & Eckel, R. H. (2017). Lipid processing in the brain: a key regulator of systemic metabolism. Front. Endocrinol. 8, 60.

46. Dietschy JM, Turley SD (2001). Cholesterol metabolism in the brain. Curr.Opin. Lipidol, 12(2)105-112.

47. Dietschy JM, (2009). Central nervous system: cholesterol turnover, brain development and neurodegeneration. Biol Chem, 390(4):287-293.

48. Petrov AM, Kasimov MR, Zefirov AL (2016). Brain cholesterol metabolism and its defects: linkage to neurodegenerative diseases and synaptic dysfunction. ActaNaturae, 8(1):58-73.

49. Mouzat K, Chudinova A, Polge A, Kantar J, Camu W, Raoul C, Lumbroso S, (2019). Regulation of brain cholesterol: what role do liver x receptors play in neurodegenerative diseases? Int J Mol Sci, 20(16):3858.

50. Villa, G. R. et al. (2016). An LXR–cholesterol axis creates a metabolic co-dependency for brain cancers. Cancer Cell 30, 683–693.

51. Tugnoli V, Tosi MR, Tinti A, Trinchero A, Bottura G, Fini G (2001) Characterization of lipids from human brain tissues by multinuclear magnetic resonance spectroscopy. Biopolymers. 62(6):297-306.

52. Wu Z, Geng F, Cheng X, Guo Q… Chakravarti A, Guo D (2020). Lipid droplets maintain energy homeostasis and glioblastoma growth via autophagic release of stored fatty acids. iScience, 23(10).

53. Taïb, B., Aboussalah, A.M., Moniruzzaman, M. et al. Lipid accumulation and oxidation in glioblastoma multiforme. Sci Rep 9, 19593 (2019). https://doi.org/10.1038/s41598-019-55985-z

54. Ioannou, M., Jackson, J., Sheu, S.-H., Chang, C.-L., Weigel, A. V., Liu, H., et al. (2018). Neuron-astrocyte metabolic coupling during neuronal stimulation protects against fatty acid toxicity. Biorxiv.

55. Guo, D., Prins, R. M., Dang, J., Kuga, D., Iwanami, A., Soto, H., Lin, K. Y., Huang, T. T., Akhavan, D., Hock, M. B., Zhu, S., Kofman, A. A., Bensinger, S. J., Yong, W. H., Vinters, H. V., Horvath, S., Watson, A. D., Kuhn, J. G., Robins, H. I., Mehta, M. P., … Mischel, P. S. (2009). EGFR signaling through an Akt-SREBP-1-dependent, rapamycin-resistant pathway sensitizes glioblastomas to antilipogenic therapy. Science signaling, 2(101), ra82. https://doi.org/10.1126/scisignal.2000446

56. Freed-Pastor W.A., Mizuno H., Zhao X., Langerod A., Moon S.H., Rodriguez-Barrueco R., Barsotti A., Chicas A., Li W., Polotskaia A., et al. Mutant p53 disrupts mammary tissue architecture via the mevalonate pathway. Cell. 2012;148:244–258. doi: 10.1016/j.cell.2011.12.017.

57. Bi, J. et al (2020). Altered cellular metabolism in gliomas – an emerging landscape of actionable co-dependency targets. Nature Reviews Cancer 20, 57-70.

58. Kant, S et al. (2020). Enhanced fatty acid oxidation provides glioblastoma cells metabolic plasticity to accommodate to its dynamic nutrient microenvironment. Cell Death and Disease, 11.

59. Strickaert A, Saiselet M, Dom G, et al. Cancer heterogeneity is not compatible with one unique cancer cell metabolic map. Oncogene. 2017;36(19):2637-2642.

60. Monteiro AR, Hill R, Pilkington GJ, Madureira PA (2017). The role of hypoxia in glioblastoma invasion. Cells, 6(4):45.

61. Velásquez C, Mansouri S, Gutiérrez O, Mamatjan Y, Mollinedo P, Karimi S, Singh O, Terán N, Martino J, Zadeh G and Fernández-Luna JL (2019) Hypoxia Can Induce Migration of Glioblastoma Cells Through a Methylation-Dependent Control of ODZ1 Gene Expression. Front. Oncol. 9:1036

62. Monteiro, A. R., Hill, R., Pilkington, G. J., & Madureira, P. A. (2017). The Role of Hypoxia in Glioblastoma Invasion. Cells, 6(4), 45. https://doi.org/10.3390/cells6040045

63. Agnihotri S, Zadeh G (2016). Metabolic reprogramming in glioblastoma: the influence of cancer metabolism on epigenetics and unanswered questions, Neuro-Oncology, 18(2): 160–172

64. Engel AJ, Lorenz NI, Klann K, Munch C, Depner C,… Luger AL. (2020). Serine-dependent redox homeostasis regulates glioblastoma cell survival. BJC. 122:1391-1398.

65. Jing K, Yang F, Shao C, Wei K, Xie M, Shen H, Shu Y. (2019). Role of hypoxia in cancer therapy by regulating the tumor microenvironment. Molecular Cancer, 18.

66. Bhattacharya S, Calar K, de la Puenta P. (2020). Mimicking tumor hypoxia and tumor-immune interactions employing three-dimensional in vitro models. J Exp Clin Cancer Res. 39(75).

67. Kucharzewska, Paulina & Christianson, Helena & Belting, Mattias. (2015). Global Profiling of Metabolic Adaptation to Hypoxic Stress in Human Glioblastoma Cells. PloS one. 10. e0116740

68. Belanger M, Allamn I, Magistretti PJ (2011). Brain energy metabolism: focus on astrocyte-neuron metabolic cooperation. Cell Metabolism, 14(6):724-738.

69. Sullivan M.R., Mattaini, K.R., Dennstedt, E.A.,… Bosenberg, M.W., Lewis, C.A., Vander Heiden, M.G. (2019) Increased Serine Synthesis Provides an Advantage for Tumors Arising in Tissues where Serine Levels are Limiting. Cell Metabolism, 30:1410-1421.

70. Davidson SM, T. Papagiannakopoulos, B.A. Olenchock, J.E. Heyman, M.A. Keibler, A. Luengo, M.R. Bauer, A.K. Jha, J.P. O'Brien, K.A. Pierce, et al (2016). Environment

impacts the metabolic dependencies of Ras-driven non-small cell lung cancer. Cell Metab., 23:517-528.

71. G.M. DeNicola, L.C. Cantley (2015). Cancer's fuel choice: new flavors for a picky eater. Mol. Cell, 60:514-523.

72. Ignatova TN, Kukekov VG, Laywell ED, Suslov ON, Vrionis FD, Steindler DA, (2002). Human cortical glial tumors contain neural stem-like cells expressing astroglial and neuronal markers in vitro. Glia, 39(3):193-206.

73. Hemmati HD, Nakano I, Lazareff JA, Masterman-Smith, M, Gaschwind DH, Bronner-Fraser M, Kornblum HI (2003). Cancerous stem cells can arise from pediatric brain tumors. PNAS, 100(25): 15178-15183.

74. Signh SK, Hawkins C, Clarke ID, Squire JA, Bayani J, … Dirks PB, (2004). Identification of human brain tumour initiating cells. Nature, 432: 396-401.

75. Cantor J.R., Abu-Remaileh M., Kanarek N., Freinkman E., Gao x., Louissaint A. Jr., Lewis C.A., Sabitini D.M. (2017). Physiologic Medium Rewires Cellular Metabolism and Reveals Uric Acid as an Endogenous Inhibitor of UMP Synthase. Cell, 169(2), 258-272.

76. Ackerman T. and Tardito S. (2019). Cell culture medium formulation and its implications in cancer metabolism. Trends Cancer. 5(6): 329-332.

77. Bardy C, van den Hurk M, Eames T, Marchand C,… Gage FH (2015). Neuronal medium that supports basic synaptic functions and activity of human neurons in vitro. Proc Natl Acad Sci USA. 112(20):2725-2734.

78. Gruetter R, Novotny EJ, Boulware SD, Rothman DL, Mason GF, Shulman GI, Shulman RG, Tamborlane WV (1992). Direct measurement of brain glucose concentrations in humans by 13C NMR spectroscopy. Proc Natl Acad Sci U S A. 89(3):1109-12.

79. Hubert CG, Rivera M, Spangler LC, Wu Q, Mack SC,… Rich JN, (2016). A three-dimensional organoid culture system derived from human glioblastomas recapitulates the hypoxic gradients and cancer stem cell heterogeneity of tumors found in vivo. Cancer Res, 76(8):2465-2477.

80. Muir A, Danai LV, Vander Heiden MG (2018). Microenvironmental regulation of cancer cell metabolism: implications for experimental design and translational studies. Disease Models and Mechanisms, 11.

81. Alquier T and Poitout V. (2017). Considerations and guidelines for mouse metabolic phenotyping in diabetes research. Diabetologia. 61:526-538.

82. Sellers K, Fox MP, Bousamra 2nd M, Slone SP,… Fan TWM, (2015). Pyruvate carboxylase is critical for non-small-cell lung cancer proliferation. J Clin Invest, 125(2):687-698.

83. Yau EH, Kummetha IR, Lichinchi G, Tang R, Zhang Y, Rana TM, (2017).Genome-wide CRISPR screen for essential cell growth mediators in mutant KRAS colorectal cancers. Cancer Res, 77(22):6330-6339.

84. Alvarez, S. W., Sviderskiy, V. O., Terzi, E. M., Papagiannakopoulos, T., Moreira, A. L., Adams, S., et al. (2017). NFS1 undergoes positive selection in lung tumours and protects cells from ferroptosis. Nature 551, 639–643.

85. Chhipa RR, Fan Q, Anderson J, Muraleedharan R, Huang Y,… Dasgupta B. (2018). AMP kinase promotes glioblastoma bioenergetics and tumour growth. Nat Cell Biol. 20(7):823-835.

86. Buck, M.D., Sowell, R.T., Kaech, S.M., and Pearce, E.L. (2017). Metabolic Instructions of Immunity. Cell. 169(4); 570-586.

87. Mukherjee P, Augur ZM, Li M, Hill C… Seyfried TN (2019). Therapeutic benefit of combining calorie-restricted ketogenic diet and glutamine targeting in late-stage experimental glioblastoma. Nature Communications Biology, 200(2).

88. G.D. Maurer, D.P. Brucker, O. Bähr, P.N. Harter, E. Hattingen, S. Walenta, W. Mueller-Klieser, J.P. Steinbach, J. Rieger (2011). Differential utilization of ketone bodies by neurons and glioma cell lines: a rationale for ketogenic diet as experimental glioma therapy. BMC Cancer, p. 315

CHAPTER 2: CDKN2A Deletion Reprograms Lipid Metabolism Priming Glioblastoma for Ferroptosis

ABSTRACT

Altered lipid metabolism is a hallmark of cancer, including in the universally lethal brain tumor glioblastoma (GBM). Efforts to exploit lipid metabolism in the treatment of GBM have been proposed, yet a requisite for this therapeutic vision is a global understanding of how distinct molecular features impact lipid composition. However, a systems-level view of the GBM lipidome is currently lacking. To identify molecular alterations underlying GBM lipid metabolic reprograming, we performed lipidomic, transcriptomic, and genomic characterization of over 200 GBM patient tumours and derivative orthotopic xenografts and gliomasphere cell cultures. Integrated analysis of genetic and transcriptomic signatures revealed that deletion of CDKN2A - altered in nearly six out of ten GBM patients - drives GBM lipid metabolic reprogramming. Loss of p16/p14 at the CDKN2A locus modulated ~25% of the GBM lipid species, affecting acyl tail length and saturation state across 13 lipid (sub) classes. One notable change in lipid composition observed in CDKN2A-deleted GBM was a significant reduction in the pool size of polyunsaturated fatty acid-containing triacylglycerides (PUFA-TAGs). Sequestration of oxidizable PUFAs into triacylglycerides (TAGs) is critical for protection from lipid oxidative cell death pathways. Accordingly, CDKN2A null GBMs exhibited markedly higher basal lipid peroxidation and increased sensitivity to ferroptosis in vitro and in orthotopic xenografts. Together, these data provide a systems-level understanding of the relationship between lipid composition and oncogenic alterations and show that loss of CDKN2A induces a unique metabolic vulnerability that can be exploited for ferroptosis-induced tumour death.

RESULTS

CDKN2A deletion rewires the GBM tumour lipidome

Molecular alterations in cancer create distinct metabolic phenotypes and, consequently, unique metabolic dependencies [1]. To identify relationships between molecular features and lipid composition, we profiled the lipidomes, transcriptomes and exomes of 114 GBM patient samples (96 bulk; 18 purified), 31 patient derived orthotopic xenografts and 52 patient-derived gliomaspheres (Figure 1 A,B). Using our GBM patient samples, we performed an unbiased Pearson correlation between tumor specific lipids (n=900, Supplementary Fig. x) and RNA gene expression. Filtered for the top 25% most highly correlated interactions (4,530 genes and 900 lipids), our analysis revealed two distinct clusters of gene-lipid associations (Figure 1C). Differential gene expression analysis between the two GBM clusters revealed Cyclin Dependent Kinase Inhibitor 2A (CDKN2A) as the most significantly different gene, followed by CDKN2B which is found at the same locus (Figure 1D) [2]. Moreover, Principal Component Analysis (PCA) of lipid species differentiated CDKN2A WT and Null GBM patient tumors as well as derivative gliomaspheres along the first principal component (Figure 1E)(Supplementary Fig. E). Lipids across all classes were altered in CDKN2A deleted compared to CDKN2A WT samples (Figure 1F). To further confirm a role for CDKN2A deletion in influencing GBM lipid composition, we genetically inhibited p14 and p16 – the two protein products of CDKN2A – using shRNA in two CDKN2A WT gliomasphere lines (Figure 1G). Lipidomic analysis revealed 25% of lipids species across numerous classes that were both significantly modulated with shp16/p14 and CDKN2A deletion in gliomasphere samples relative to parental controls (Figure 3F,H). Together, these data indicate that CDKN2A deletion, found in ~60% of GBM patients, regulates GBM lipid metabolism.

CDKN2A Deletion Increases Lipid Peroxidation and Ferroptosis in GBM

Triacylglycerides (TAGs) represented 61% of the lipid species that were altered with CDKN2A deletion (Figure 2A). Specifically, CDKN2A Null GBMs consisted of significantly fewer polyunsaturated fatty acids (PUFA) TAGs, while having elevated saturated fatty acids (SFA) and monounsaturated fatty acid (MUFA) TAGs, relative to CDKN2A WT samples (Fig. 2A). PUFAs in cellular membranes are more sensitive to lipid peroxidation than SFAs or MUFAs due to the presence of multiple double bonds which facilitate hydrogen abstraction and lipid peroxidation from reactive oxygen species [3]. PUFAs sequestered into lipid droplets, the major store of TAGs in the cell, can be protected from lipid peroxidation [4]. Intriguingly, quantification of lipid peroxidation using the 581/591 C11 BODIPY revealed greater basal lipid peroxidation in CDKN2A Null compared to WT gliomaspheres (Figure 2B). p14/p16 knockdown in two CDKN2A WT gliomaspheres mirrored both the decrease in PUFA TAG composition (Figure 2A), as well as the increase in basal lipid peroxidation found in CDKN2A deleted tumors (Figure 2C). Thus, reduced PUFA TAG levels with CDKN2A loss is coupled to increases in lipid peroxidation in GBM.

Ferroptosis mediated cell death can be triggered by the lethal accumulation of PUFA peroxides [5]. Therefore, we posited that the heightened basal lipid peroxidation observed in CDKN2A deleted gliomaspheres may sensitize these tumors to ferroptosis. Inhibition of glutathione peroxidase 4 (GPX4) with ((1S,3R)-RSL3) or ML210 caused pronounced cell death across a panel of CDKN2A null gliomaspheres while, conversely, CDKN2A WT gliomaspheres were largely tolerant to the drug (Figure 2F,G and Supplemental Fig 2F). Consistent with the selective susceptibility of CDKN2A deleted GBMs to lethal lipid peroxidation, GPX4 inhibition

increased lipid peroxidation only in CDKN2A null gliomaspheres (Figure 2E). Moreover, the addition of ferrostatin-1 (Fer-1), liproxstatin-1 (Lip-1), or the iron chelator deferoxamine (DFO) – all canonical inhibitors of ferroptosis (Figure 2H) – mitigated cell death with GPX4 inhibition. Finally, genetic knockdown of p14/p16 increased lipid peroxidation sensitivity and ferroptosis in response to RSL3 (Figure 2I). Together, these data indicate that CDKN2A null GBM are more susceptible to ferroptosis relative to CDKN2A WT GBM.

CDKN2A deletion impacts the sequestration of oxidizable PUFA into lipid droplets

We next sought to understand the mechanism by which CDKN2A deletion renders GBMs susceptible to ferroptosis. With CDKN2A intact, we observed a significant enrichment in PUFA TAGs containing arachidonic acid (AA), adrenic acid, (AdA) and docosapentaenoic acid (DPA) acyl tail moieties (Supplemental Figure 2B). Oxidation of AA esterified to phosphatidylethanolamine (PE) phospholipids contributes to the execution of ferroptosis [6]. Therefore, we hypothesized that sequestration of AA into TAGs selectively protects CDKN2A WT GBM against lipid peroxidation and ferroptosis. Accordingly, CDKN2A WT (n=3) and Null gliomaspheres (n=3) were incubated with AA for 24 hours and the resulting changes in lipid composition were quantified with shotgun lipidomics analysis. Exogenous AA led to increased PUFA-containing TAG composition in CDKN2A WT gliomaspheres. Conversely, the addition of AA to CDKN2A Null gliomaspheres caused an expansion in AA-containing PE phospholipid pools (Figure 3A). DGAT1 and DGAT2 are the two rate-limiting enzymes that convert diacylglycerides to triacylglycerides in the endoplasmic reticulum [7]. Co-treatment with DGAT1 and DGAT2 inhibitors completely inhibited the formation of TAGs in both CDKN2A WT and Null gliomaspheres, normalizing the differences in PUFA lipid composition (Figure 3A). As TAGs

are the major components of lipid droplets, we sought to observe lipid droplet synthesis under the same conditions of exogenous arachidonic acid addition. In agreement with our observations, lipid droplet area was significantly increased in CDKN2A WT gliomaspheres in response to exogenous arachidonic acid compared to CDKN2A Null gliomaspheres (Figure 3B). DGAT1 and DGAT2 inhibition completely prevented the increase in lipid droplets in both CDKN2A WT and Null gliomaspheres. These data suggest that CDKN2A Null gliomaspheres are deficient in their ability to incorporate exogenous arachidonic acid into TAGs and lipid droplets.

We next aimed to connect the sequestration of arachidonic acid into lipid droplets to the resistance to lipid peroxidation and ferroptosis in CDKN2A WT GBM. Lipid peroxidation was increased with exogenous arachidonic acid and RSL3 in CDKN2A Null gliomaspheres more than in CDKN2A WT (Figure 3C). However, DGAT1 and DGAT2 inhibition increased lipid peroxidation in CDKN2A WT more than in Null gliomaspheres. We next sought to determine if DGAT1 and DGAT2 play a role in ferroptosis resistance. CDKN2A WT gliomaspheres (n=3) showed a significant increase in cell death with DGAT1 and DGAT2 inhibition when co-treated with arachidonic acid and RSL3, while CDKN2A Null gliomaspheres (n=3) had already achieved maximal cell death with RSL3 and arachidonic acid alone (Figure 3D). This result indicates the protective role of PUFA TAG composition in CDKN2A WT resistance to ferroptosis. Supporting this finding, combined p14 and p16 knockout decreased arachidonic acid-induced lipid droplet accumulation (Figure 3E) and reduced the DGAT1 and DGAT2-mediated lipid peroxidation and ferroptosis protection (Figure 3E, F). This finding highlights a novel role of CDKN2A in the sequestration of PUFAs into TAGs and subsequent protection against ferroptosis.

GPX4 inhibition decreases tumour burden in CDKN2A Null GBM orthotopic xenografts

Given the conservation of the CDKN2A-dependent lipidome in vivo (Figure 4A), we hypothesized that ferroptosis sensitivity in vitro would be preserved within the brain tumour microenvironment. Quantification of the lipid peroxidation by-product malondialdehyde (MDA) in orthotopic mouse xenograft GBM tumour tissues using immunofluorescent microscopy revealed higher MDA levels in CDKN2A Null tumours compared to CDKN2A WT tumours (Figure 4B). To test the sensitivity of orthotopic xenograft tumours to ferroptosis with GPX4 inhibition, we used CRISPR/Cas9-to knockout GPX4 expression in CDKN2A WT and Null gliomaspheres (Figure 4C). In vitro validation showed sensitivity to ferroptosis upon GPX4 knockout in CDKN2A Null gliomaspheres (Supplemental Figure 4C). Cells were transduced, selected, and immediately injected orthotopically into NOD scid gamma (NSG) mice to generate GBM tumours. CDKN2A Null xenografts had increased overall survival with GPX4 knockout (Figure 4E). GPX4 protein expression was regained and Cas9 expression was lost in the collected GPK4 knockout xenograft tumors, suggesting the outgrowth of GPX4 WT cells in these tumors (Supplemental Figure 4F). Our results indicate that CDKN2A Null GBM exhibit increased lipid peroxidation in vivo, and are susceptible to ferroptosis with GPX4 inhibition in vivo. The conservation of the CDKN2A-dependent phenotype in orthotopic xenograft models of GBM indicates the potential translatability of these findings.

DISCUSSION

Here, we have comprehensively characterized the GBM-intrinsic lipidome and identified a novel role of CDKN2A in modulating lipid metabolism in GBM. Our observation that CDKN2A

deletion leads to extensive lipid composition remodeling in GBM across diverse tumor microenvironments is a novel role for this gene overall as well as in the context of GBM. Future studies should aim to determine if CDKN2A deletion alters lipid composition across other cancer types. CDKN2A deletion is a common alteration across many cancers and may therefore have similar effects on lipid metabolic reprograming. Alternatively, the tumor cell of origin may shape this metabolic dependency and make this a GBM-specific phenomenon.

The brain is uniquely predisposed to lipid peroxidation due to high neuronal ATP demand and elevated levels of oxygen uptake [8]. As a result, the brain consumes 20% of available oxygen and is vulnerable to the accumulation of reactive oxygen species [9]. Additionally, neuronal membranes are enriched in arachidonic acid and docosahexaenoic acid, two PUFAs that are sensitive to lipid peroxidation. Particularly critical for ferroptosis, multiple regions of the brain are enriched in iron, which further increases with age [10]. In order to prevent damaging lipid peroxidation and resulting neurodegeneration, the brain needs to tightly regulate antioxidant mechanisms. Therefore, it is reasonable to hypothesize that the within the brain tumor microenvironment, GBM tumors would be very sensitive to lipid peroxidation in response to GPX4 inhibition, presenting a potential therapeutic opportunity.

Finally, this work has identified a role of CDKN2A in altering the GBM lipidome, However the specific mechanisms by which p14 and or p16 regulate lipid metabolic pathways is yet to be fully elucidated. Future studies will identify the molecular mechanisms by which PUFA TAG composition is altered. Additionally, further investigation of this dataset will explore additional molecular alterations and their impact of the GBM lipidome.

FIGURES AND TABLES

Chapter 2 – Figure 1

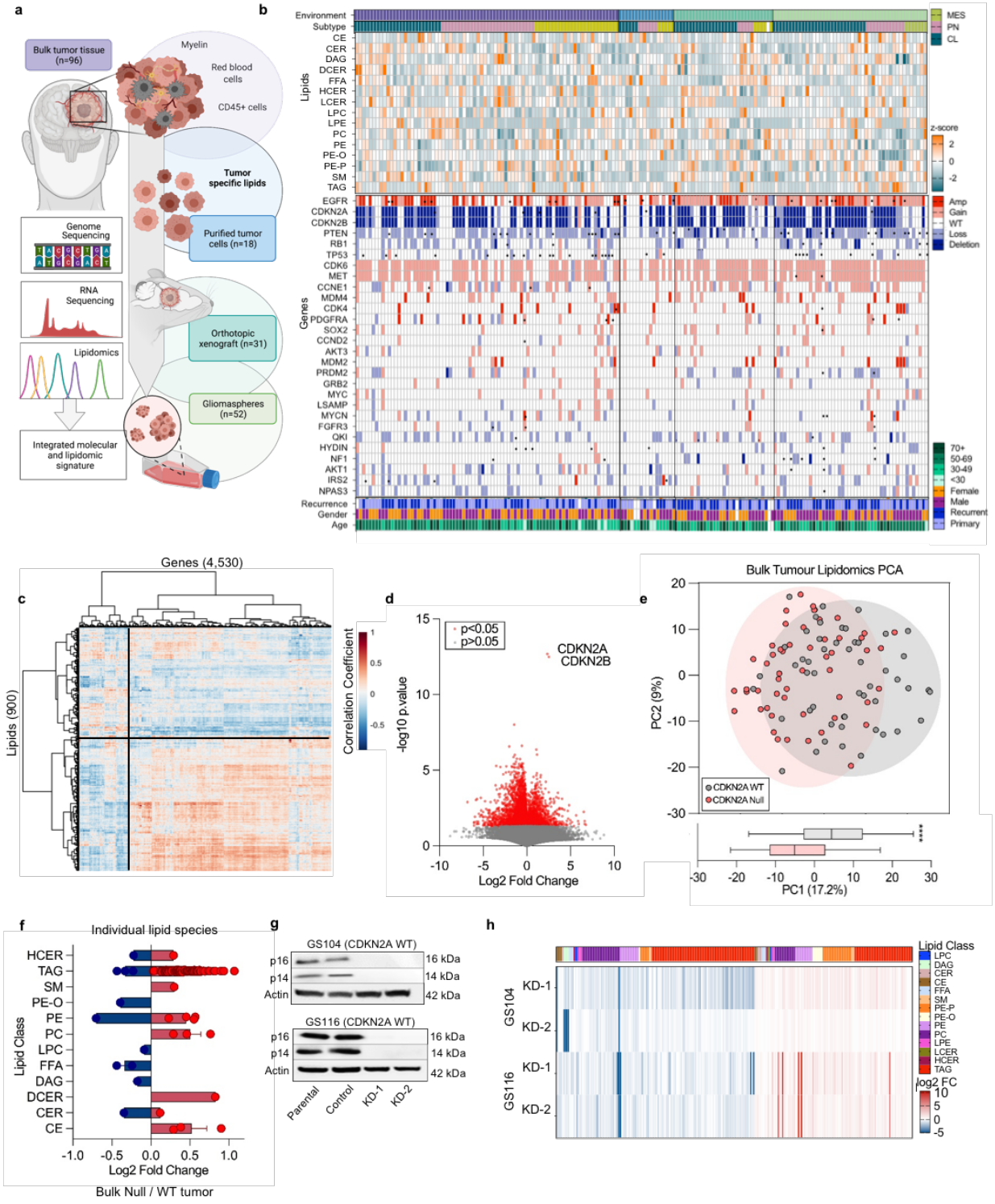

Figure 1. Comprehensive characterization of the GBM lipidome reveals the impact of CDKN2A deletion across tumor microenvironments. (A) Graphical abstract of our approach to collect patient tumor samples and perform RNA and whole exome sequencing and lipidomics across tumor microenvironments. (B) Plot depicting tumor microenvironment type (from left to right – bulk tumor tissue, purified tumor cells, orthotopic xenografts, and gliomaspheres), tumor subtype, lipid class composition, copy number alterations and mutations frequently occurring in GBM, tumor recurrence, patient age, and gender. Lipid composition is plotted as a z-score across samples within a tumor microenvironment type. (C) Pearson correlation matrix of lipid composition and RNA expression. The top 25% most highly correlated gene-lipid associations are shown (4,530 genes and 900 lipids). (D) Volcano plot showing differential gene expression between the two GBM groups. CDKN2A and CDKN2B are the most significantly differentially expressed genes between the two groups. (E) Principal Component Analysis of lipid species differentiates CDKN2A WT and Null neurospheres along Principal Component 1 (20.2 % of variance). (F) CDKN2A deletion alters lipid composition across lipid classes. (G) Immunoblot of shRNA-mediated knockout of p14 and p16 in two CDKN2A WT gliomaspheres. (H) Knockout of p14 and p16 induces lipid alterations also observed in CDKN2A deleted GBM tumor tissues. MES: mesenchymal, PN: proneural, CL: classical.

Chapter 2 – Figure 2

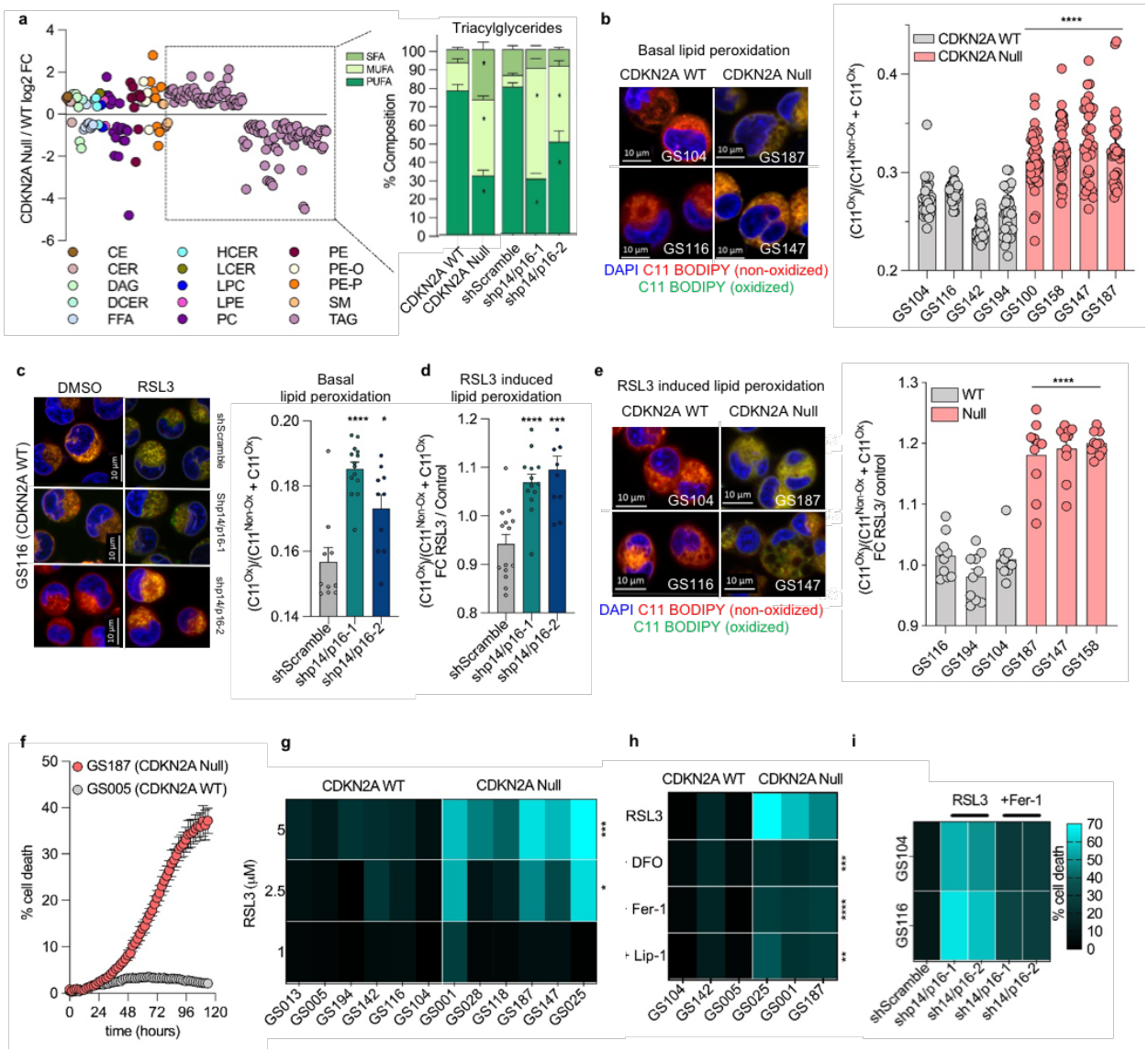

Figure 2: CDKN2A null GBM are more susceptible to lipid peroxidation and ferroptosis. (A) Log2 fold change of significantly altered lipids in CDKN2A Null compared to CDKN2A WT gliomaspheres. CDKN2A Null and p14/p16-deleted gliomaspheres have a significant decrease in PUFA TAGs. (B) CDKN2A Null neurospheres (n=4) have a higher lipid peroxidation signal with C11 BODIPY 581/591 lipid peroxidation probe than CDKN2A WT neurospheres (n=4). (C) Knockout of p14 and p16 in CDKN2A WT GS116 increased lipid peroxidation basally and (D) in response to the GPX4 inhibitor RSL3 (24 hours at 2.5 μM). (E) CDKN2A Null neurospheres have higher lipid peroxidation in response to treatment with RSL3 (F) Representative trace of cell death over time from the Incucyte live cell imaging system with CellTOX cell death reagent. Percent cell death is calculated as the percent of green objects (dead cells) out of total red objects (cell nuclei). CDKN2A Null (GS187) are more sensitive to cell death with 2.5 μM RSL3 treatment compared to CDKN2A WT GS005. (G) Summary of percent cell death across three doses of RSL3 shows significantly more death in CDKN2A Null neurospheres with 2.5 and 5 μM RSL3. (H) Canonical ferroptosis inhibitors (DFO, Ferrostatin-1, and Liproxstatin-1) significantly rescue cell death. (I) Knockout of p14 and p16 in two CDKN2A WT neurospheres increases cell death compared to Scramble control. Cell death is partially rescued with Ferrostatin-1 (1 μM).

Chapter 2 – Figure 3

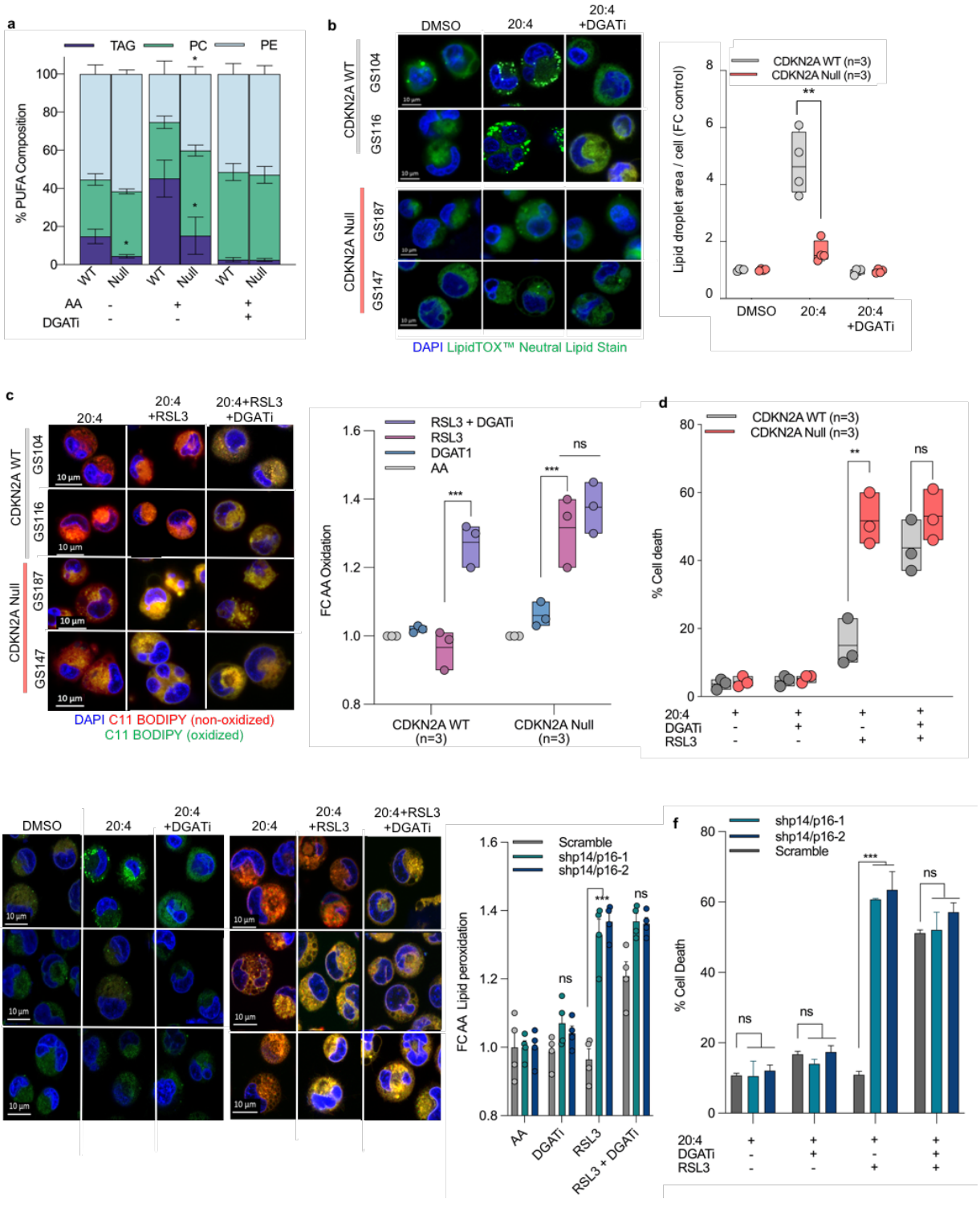

Figure 3: CDKN2A deletion impacts the sequestration of oxidizable PUFA into LD priming GBM for ferroptosis (A) Arachidonic acid increased PUFA TAGs in CDKN2A WT neurospheres (n=3) but increased PUFA PE in CDKN2A Null samples (n=3). DGAT1 and DGAT2 inhibition prevented the effect. (B) Arachidonic acid increased lipid droplet area in CDKN2A WT neurosphere (n=4) but not CDKN2A Null (n=4). DGAT1 and DGAT2 inhibition prevented the effect. (C) Co-treated with arachidonic acid and RSL3 increases lipid peroxidation in CDKN2A Null gliomaspheres. DGAT1 and DGAT2 inhibition sensitized only the CDKN2A WT cells to enhanced lipid peroxidation. (D) DGAT1 and DGAT2 inhibition sensitized only CDKN2A WT neurospheres to ferroptosis in the presence of RSL3 and arachidonic acid. (E) Sensitivity to lipid peroxidation in CDKN2A WT neurospheres with p14 and p16 knockdown replicate the observation in CDKN2A WT and Null neurospheres. (F) Knockdown of p14 and p16 increases sensitivity to cell death with RSL3 and arachidonic acid.

Chapter 2 – Figure 4

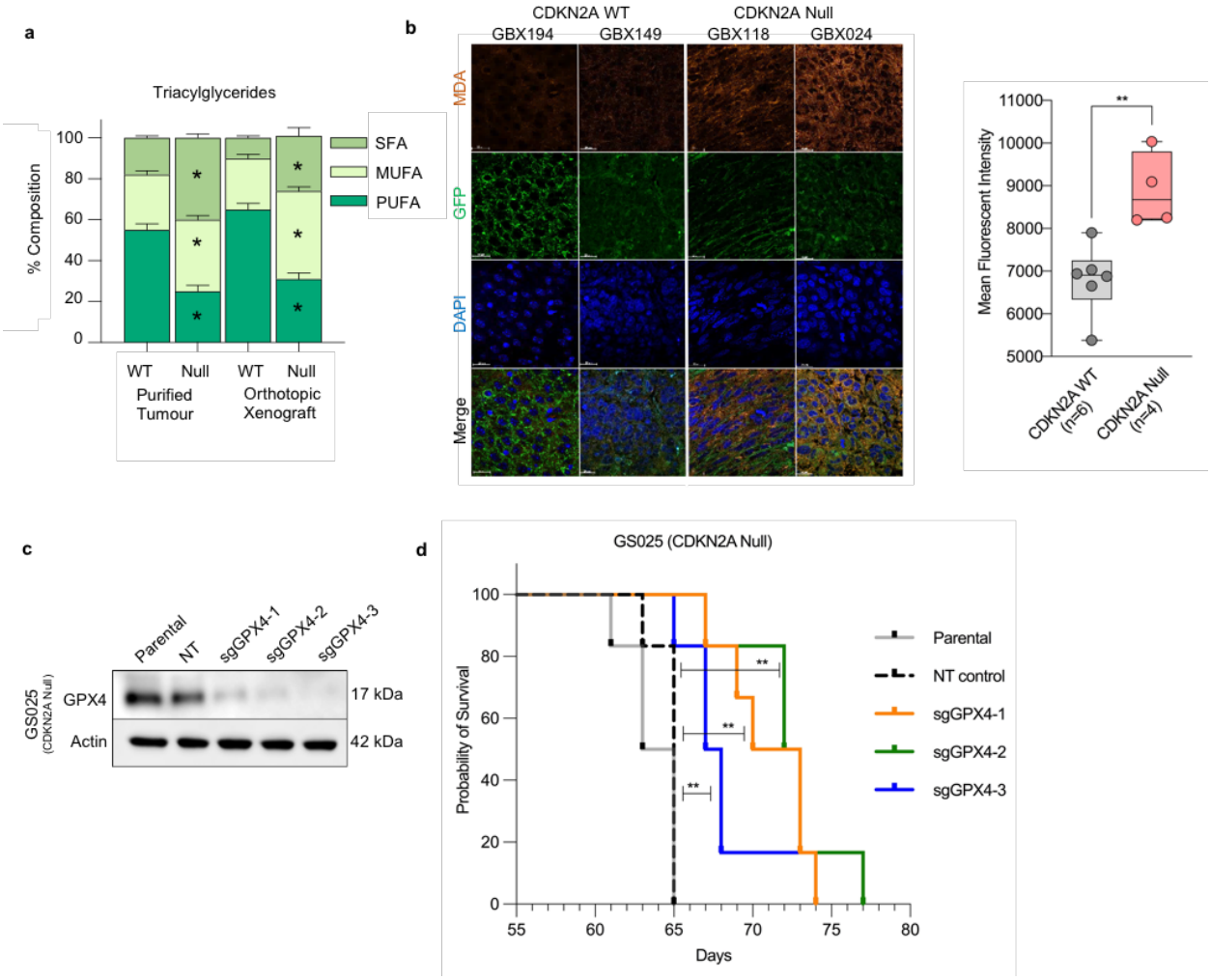

Figure 4: CDKN2A Null GBM have higher basal peroxidation and are more sensitive to GPX4 inhibition than CDKN2A WT orthotopic xenograft tumors. (A) In purified tumors (n=18) and orthotopic xenografts (n=31) PUFA TAGs are significantly decreased in CDKN2A Null GBM, while saturated (SFA) and monounsaturated fatty acids (MUFAs) are significantly increased. (B) MDA mean immunofluorescence intensity is quantified in CDKN2A WT and Null orthotopic xenograft tumor tissues reveals significantly higher MDA levels in CDKN2A Null tumors. (C) Immunoblot of GPX4 knockout efficiency with CRISPR/Cas9 in the CDKN2A Null gliomasphere GS025. Three separate guides for GPX4 are used. D) CDKN2A Null orthotopic xenografts with GPX4 knockout had a significant overall survival benefit compared to the non-targeting control and parental cell line xenografts (n=6 mice per group).

SUPPLEMENTARY FIGURES

Chapter 2 – Supplemental Figure 1

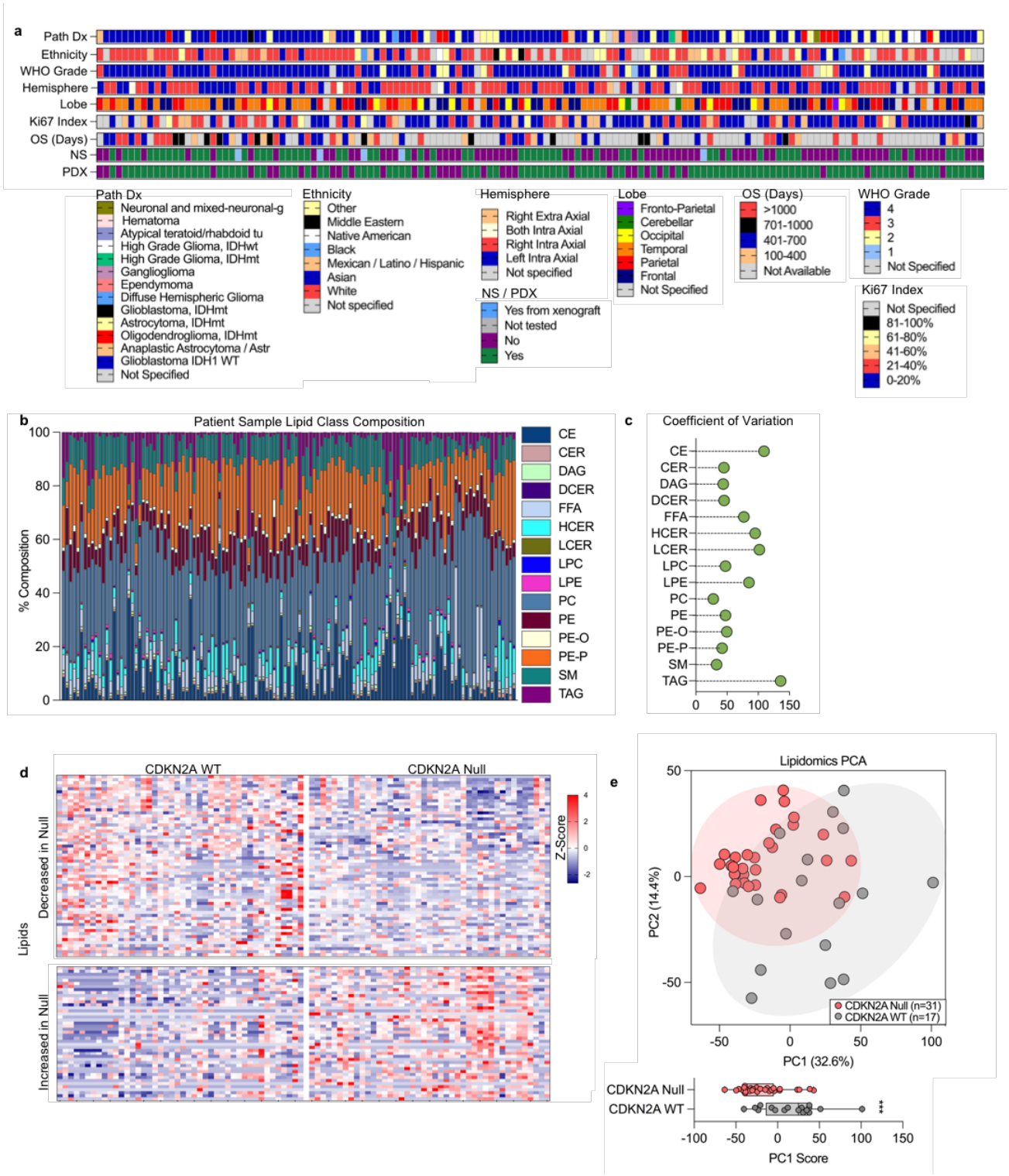

Supplemental Figure 1: (A) Additional patient data is depicted. Diagnosis (Path Dx), patient ethnicity, tumor hemisphere and lobe location, WHO grade, Ki67 Index value, and overall survival (OS) are shown. The presence of a derivative gliomasphere (NS) and orthotopic xenograft (PDX) are indicated. (B) A plot displays the lipid class composition across 114 GBM tumors (C) The coefficient of variation across samples is plotted per lipid class. (D) GBM tumor lipid composition differences are displayed with z-scores of 104 significantly different lipids in CDKN2A WT and Null tumors. (E) Principal component analysis of gliomaspheres (n=48) shows 32.6% of variance explained by principal component 1 and significant differences between WT and Null groups.

Chapter 2 – Supplemental Figure 2

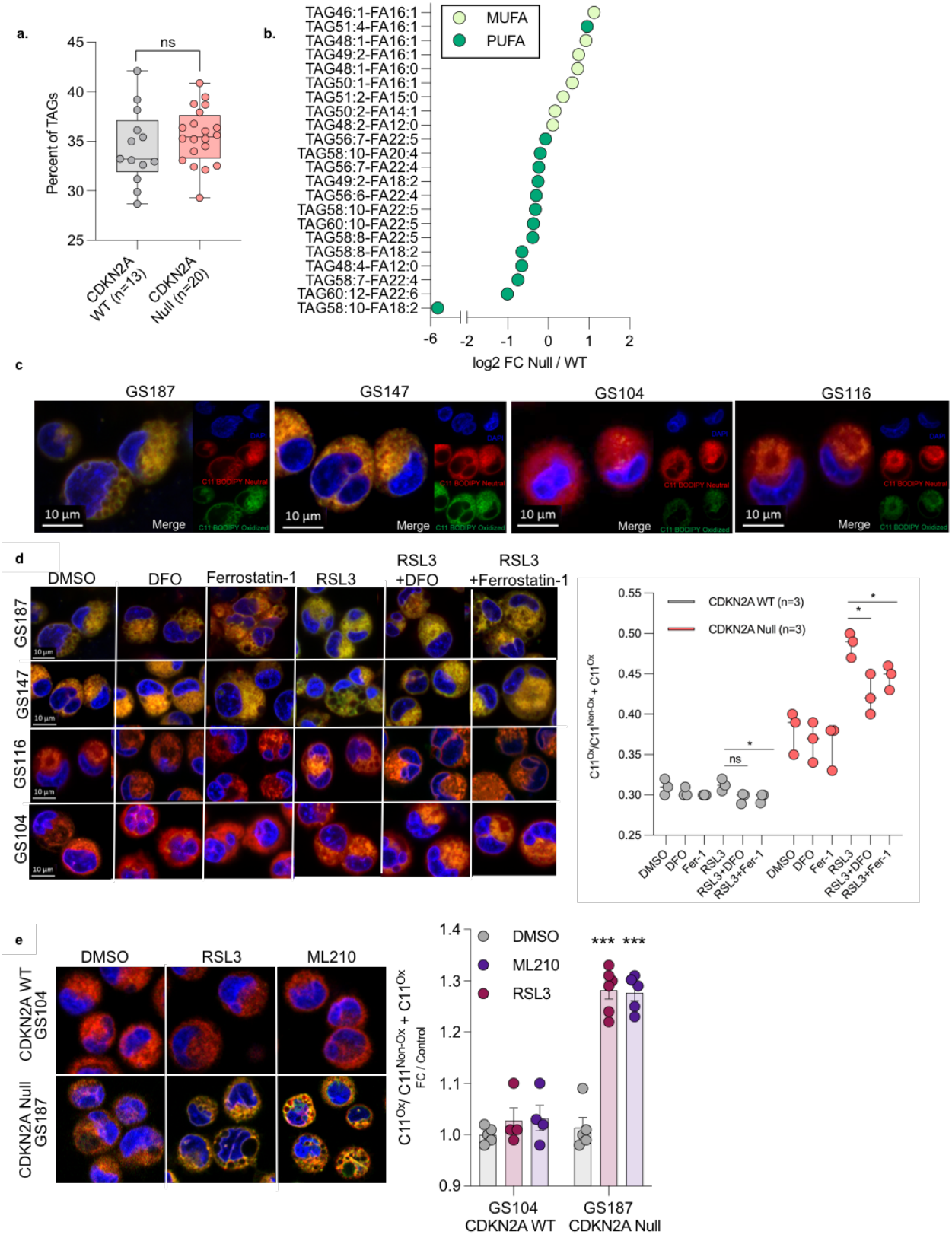

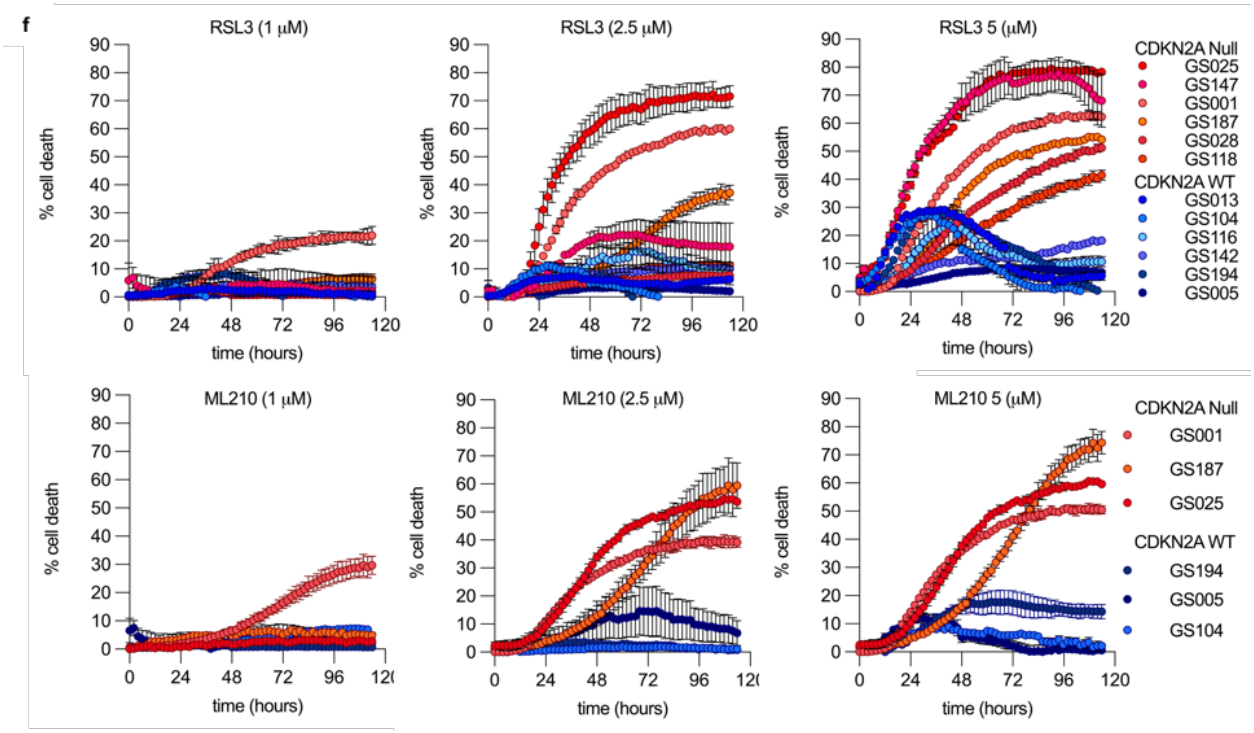
f
RSL3 (1 μM)
RSL3 (2.5 μM)
RSL3 5 (μM)
ML210 (1 μM)
ML210 (2.5 μM)
ML210 5 (μM)
% cell death
time (hours)
CDKN2A Null
GS025
GS147
GS001
GS187
GS028
GS118
CDKN2A WT
GS013
GS104
GS116
GS142
GS194
GS005

Supplemental Figure 2. (A) Quantification of percent of TAG lipids altered in CDKN2A WT and Null gliomaspheres indicates no significant change overall. (B) A species-level view of significantly altered lipids across all tumor microenvironments reveals plotted as log2 fold change CDKN2A Null over WT. MUFA TAGs are generally enriched and PUFA TAGs are decreased in CDKN2A Null GBM. (C) Images of lipid peroxidation with separate channels in 4 representative cell lines. Blue: DAPI, Green: oxidized C11 BODIPY, Red: non-oxidized C11 BODIPY probe. (D) All additional lipid peroxidation controls with images and corresponding quantification. (E) The GPX4 inhibitor ML210 induces more lipid peroxidation in GS187 (CDKN2A Null) gliomasphere compared to GS104 (CDKN2A WT). (F) Percent cell death is quantified by the Incucyte live cell imaging system with increasing doses of RSL3 and ML210. CDKN2A Null gliomaspheres are more sensitive to cell death in response to both compounds compared to CDKN2A WT gliomaspheres.

Chapter 2 – Supplemental Figure 3

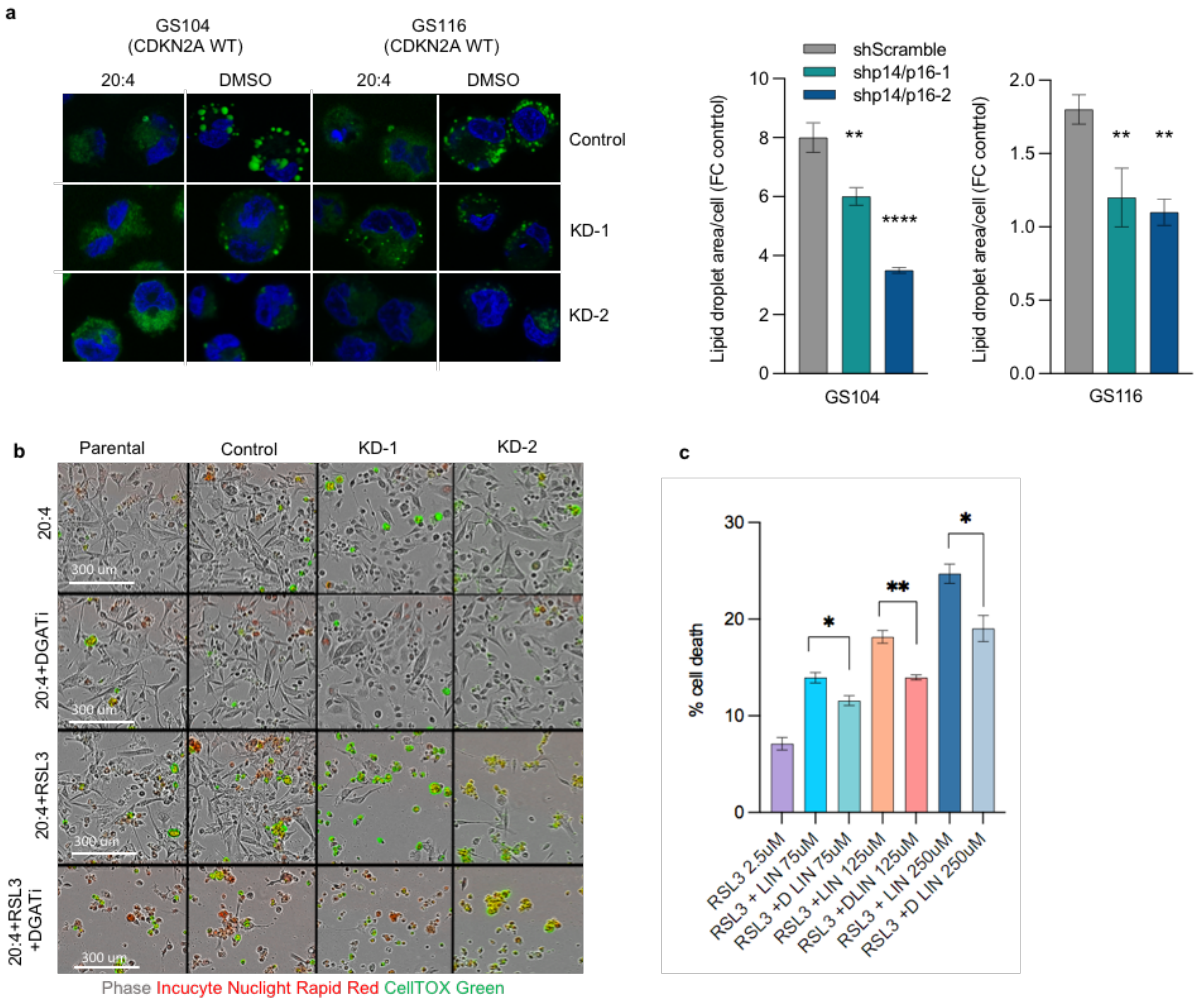

Supplemental Figure 3. (A) Fluorescent imaging of lipid droplets (green) and cell nuclei (blue) in CDKN2A WT gliomaspheres GS104 and GS116 and two respective p14/p16 knockdown cell lines are shown. Quantification of lipid droplet area per cell (fold change of control) shows decreased lipid droplet area in p14/p16 knockdown cell lines. (B) Incucyte images of cell death (green) and cell nuclei (red) in response to treatment with arachidonic acid, DGAT1/2 inhibition, and RSL3. (C) Percent cell death in gliomaspheres treated with linolenic vs deuterated-linolenic acid shows a significant survival benefit with the deuterated fatty acid.

Chapter 2 – Supplemental Figure 4

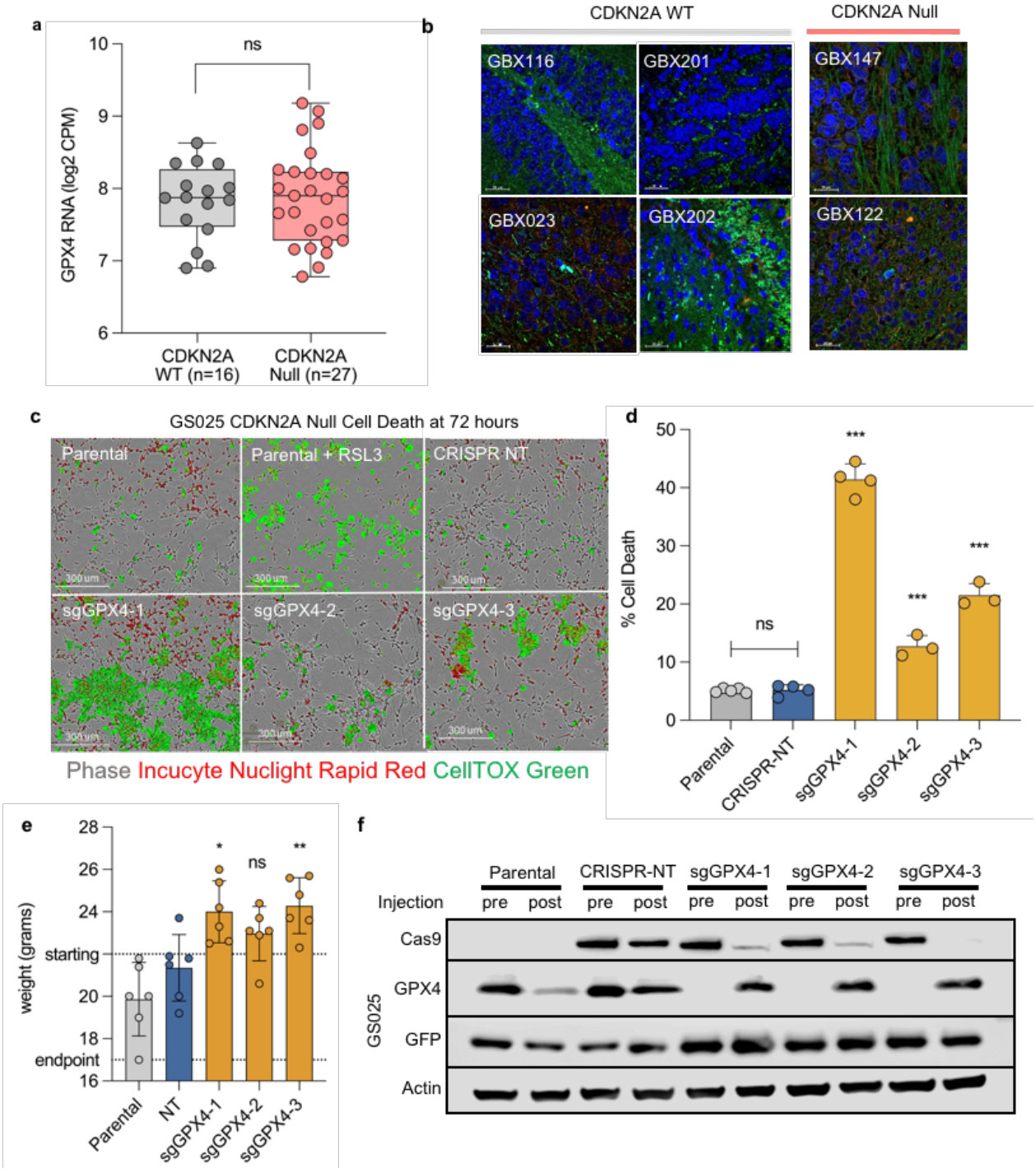

Supplemental Figure 4. (A) GPX4 RNA expression (log2 CPM) is not significantly different between CDKN2A WT and Null gliomaspheres. (B) MDA immunofluorescent staining of additional CDKN2A WT and Null sphere-derived orthotopic xenograft tumors. (C) Incucyte images at 72 hours incubation of cell number and cell death in response to GPX4 knockout in the CDKN2A Null gliomasphere GS025. CellTOX (green) signal indicates cell death and Nuclight Rapid (red) signal indicates the cell nucleus. (D) Quantification of percent cell death from Incucyte images. (E) Weight in grams of each mouse (n=6 per group) after tumor burden is achieved shows decreased body mass in the non-targeting control (NT) and parental cell line (parental) xenografts compared to the GPX4 knockout xenografts. Statistics performed between GPX4 knockout lines and NT condition. (F) Immunoblot of cells before injection and isolated xenograft tumors post injection indicates the expression of GPX4 and loss of Cas9 in the resected tumors.

EXPERIMENTAL METHODS

Mice. Female NOD *scid* gamma (NSG) mice, 6–8 weeks of age, were purchased from the University of California Los Angeles (UCLA) Medical Center animal-breeding facility and Jackson Laboratories. All mice were kept under defined pathogen-free conditions at the AAALAC-approved animal facility of the Division of Laboratory Animals (DLAM) at UCLA. All animal experiments were performed with the approval of the UCLA Office of Animal Resource Oversight (OARO).

Patient-derived GBM tumors. After explicit informed consent was obtained from patients, all patient tissue used to derive GBM cell cultures was obtained through the UCLA Institutional Review Board (IRB) protocol 10-000655. Tumors were mechanically and enzymatically dissociated using the Miltenyi Biotec Human tumor dissociation kit. Red blood cell lysis buffer removed red blood cells. Antibody-conjugated magnetic beads removed CD45+ cells and myelinated cells in two column-based filtration steps. Primary GBM cells were established and maintained in gliomasphere conditions consisting of DMEM/F12 (Gibco), B27 (Invitrogen), penicillin–streptomycin (Invitrogen), and GlutaMAX (Invitrogen) supplemented with heparin (5 μg/mL, Sigma), EGF (50 ng/mL, Sigma), and FGF (20 ng/mL, Sigma). All cells were grown under 37 °C, 20% O_2, and 5% CO_2 and were routinely monitored and tested negative for the presence of mycoplasma with a commercially available kit (MycoAlert, Lonza). Gliomasphere cell lines were used at fewer than 15 passages. All cells were authenticated by short tandem repeat (STR) analysis.

Gliomasphere-derived orthotopic xenografts. To produce neurosphere-derived orthotic xenografts tumors, gliomaspheres were transduced with the Gaussia-luciferase reporter to enable

non-invasive quantification of tumor burden as well as endpoint GFP-guided microdissection of the tumor tissue from the surrounding normal brain [11]. Gliomaspheres were dissociated and injected (5 x10^4 cells per injection) into the right striatum of the brain in femal NSG mice (8-9 weeks old). Injection coordinates were 2mm lateral and 1mm posterior to bregma, at a depth of 2mm. Tumor burden was monitored on the basis of secreted Gaussia luciferase.

Secreted Gaussia luciferase measurements. Cells were infected with a lentiviral vector containing a secreted Gaussia luciferase (sGluc)-encoding reporter gene (Targeting Systems no. GL-GFP) and intracranially implanted into the right striatum in mice (4 × 105 cells/mouse). To measure the levels of secreted Gaussia luciferase (sGluc), 6 μL of blood was collected from the tail vein and immediately mixed with 50 mM EDTA to prevent coagulation. Gluc activity was obtained by measuring chemiluminescence after injection of 100 μL of 100 μM coelentarazine (Nanolight) in a 96-well plate, as described before

Genetic manipulations. Lentivirus particles used for genetic manipulation were produced by transfection of 293-FT cells (Thermo) with Lipofectamine 2000 (Invitrogen). Virus particles were collected 48 h after transfection. The shRNA guide sequences used to knockdown p14 and p16 TRCN0000255853 and TRCN0000255849 in the Vector backbone pLKO. CRISPR/Cas9 HDR was used to knockout p14 and p16 using pHDR-CDKN2A-Ex2-CMV-EGFP (Addgene 1107342), pEN35-CDKN2A-Ex2-L (Addgene 1107363) and pEN35-CDKN2A-Ex2-R (Addgene 110737)[12]. GPX4 CRISPR/Cas9 knockout was performed with the LentiCRISPR V2 vector using TRCN0000304065, TRCN0000046252, and TRCN0000046248.

Reagents and antibodies. Chemical inhibitors from the following sources were dissolved in DMSO for *in vitro* studies: RSL3, ML210, Ferrostatin-1, DFO, and Liproxstatin-1. The following antibodies were obtained from the indicated sources and used for immunoblotting: p16 INK4A (D3W8G) Rabbit mAb #928033 (Cell Signaling), p14 ARF (4C6/4) Mouse mAb#2407 (Cell Signaling), α-GPX4 (Cell Signaling), α-Actin (Cell Signaling)., Cas9 (7A9-3A3) Mouse mAb #14697 (Cell Signaling). Antibodies used for immunoprecipitation were obtained from the following sources: α-MDA,

Immunoblotting. Cells were collected and lysed in RIPA buffer (Boston BioProducts) containing Halt Protease and Phosphatase Inhibitor (Thermo Fisher Scientific). Lysates were centrifuged at 14,000*g* for 15 min at 4 °C. Protein samples were then boiled in NuPAGE LDS Sample Buffer (Invitrogen) and NuPAGE Sample Reducing Agent (Invitrogen), separated with SDS–PAGE on 12% Bis-Tris gels (Invitrogen) and transferred to nitrocellulose membranes (GE Healthcare). Immunoblotting was performed per the antibody manufacturers' specifications, as mentioned previously. Membranes were developed with the SuperSignal system (Thermo Fisher Scientific).

Shotgun Lipidomics. Shotgun lipidomic analysis was performed using direct infusion-tandem mass spectrometry utilizing a differential mobility system. The assay was performed on the SCIEX 5500 triple-quadrupole with a Shimadzu auto-sampler, SelexION ion mobility device, and Shimadzu LC and utilized the Sciex Lipidyzer Platform. 70 lipid standards enabled detection of over 1,040 unique lipid species across 13 lipid classes.

Quantifying lipid peroxidation with BODIPY 581/591 C11. Lipid peroxidation was assessed using the lipid peroxidation probe BODIPY 581/591 C11 from Thermo Fisher. This lipid analog is rapidly incorporated into the membranes of living cells. The probe undergoes a conformational change once oxidized, shifting from red fluorescence in the reduced form to green in the oxidized form. To assess lipid peroxidation in vitro, gliomaspheres were split and cultured for 24 hrs in previously described neurosphere medium except the B-27 is without antioxidants. After 24 hrs, the cells were collected, dissociated with trypsin, and re-suspended as single cells in Hank's Buffered Salt Solution (HBSS) containing the BODIPY 581/591 C11 (1:1000) and Hoechst nuclear stain (1:1000). Cells were incubated for 15 minutes in the dark in solution on a Cell-tak treated coverslip to enable cell adhesion. Coverslips were then washed once in HBSS and inverted onto a slide with 100ul HBSS and parafilm spacers, and then sealed with valap to enable live cell confocal microscopy. Images were acquired on a confocal LSM880 microscope at 63x magnification.

Cell death kinetics. Opaque-sided clear bottomed 96-well plates were laminin-coated for 1 hour and then washed two times with neurobasal media. Gliomaspheres were dissociated into single cell suspension, filtered, plated at 20,000 cells per well, and allowed to attach for 4 to 12 hours. Once cells were attached, media was briefly removed and replaced with antioxidant-free media containing CellTOX cell death green fluorescent dye (1:1000) (Promega) and nuclear red fluorescent dye (1:1000) (Incucyte) as well as the required compounds. The plate was then set in an Incucyte live-cell imaging system which captured images every 2 hours for up to five days. Incucyte software image analysis was performed using top-hat image normalization, and percent cell death was calculated using percentage of green objects/mm^2 over red objects/mm^2.

Quantifying MDA levels with TBARs. The TBARs assay kit (Cayman Chemical) was used following kit instructions. Cell lysates and tumor tissues were sonicated and the lysate was used to determine MDA concentration, which was normalized to protein concentration from the same lysate. Samples were mixed with color reagent and boiled for one hour in 15ml conical tubes. Fluorometric assay readout was used for the cell lysates. Colorimetric readout was used for the tissue lysates due to the high concentration of MDA present.

Quantifying MDA levels with immunofluorescent microscopy. Tumor tissues were PFA-fixed and paraffin-embedded, and slices were mounted onto slides. Slides were de-paraffinized and antigen-retrieval was performed. MDA primary (Abcam cat#) was incubated overnight at 4 degrees C with 1:500 goat anti-MDA primary antibody followed by secondary incubation with donkey anti-goat Alexa 647.

Lipid droplet quantification. Lipid droplets were assessed using HCS LipidTOX™ Deep Red neutral lipid dye. Cells were collected and trypsinized following standard procedure for neurosphere cultures. The cell pellet was then re-suspended in media containing the LipidTOX™ dye (1:1000). Cells were distributed onto a coverslip pre-treated with Cell-tak to enable rapid cell adhesion. Cells were allowed to attach to the coverslip for 30 minutes before the addition of PFA to fix the cells. Coverslips were washed in HBSS and then water and mounted onto a slide using Invitrogen Prolong Gold Antifade mounting reagent with DAPI. Confocal microscopy on the LSM880 microscope at 63x magnification was used to capture the lipid droplet and DAPI stains. Lipid droplet area and number per cell was quantified using ImageJ FIJI.

REFERENCES

1. Strickland, M. & Stoll, E. A. Metabolic reprogramming in glioma. Front. Cell Dev. Biol. 5, 43 (2017).

2. Foulkes, W. D., Flanders, T. Y., Pollock, P. M. & Hayward, N. K. The CDKN2A (p16) gene and human cancer. Mol. Med. 3, 5–20 (1997).

3. Ayala, A., Muñoz, M. F. & Argüelles, S. Lipid peroxidation: production, metabolism, and signaling mechanisms of malondialdehyde and 4-hydroxy-2-nonenal. Oxid. Med. Cell. Longev. 2014, (2014).

4. Jarc, E. & Petan, T. Focus: Organelles: Lipid droplets and the management of cellular stress. Yale J. Biol. Med. 92, 435 (2019).

5. Dixon, S. J. & Stockwell, B. R. The hallmarks of ferroptosis. Annu. Rev. Cancer Biol. 3, 35–54 (2019).

6. Kagan, V. E. et al. Oxidized arachidonic and adrenic PEs navigate cells to ferroptosis. Nat. Chem. Biol. 13, 81–90 (2017).

7. Yen, C.-L. E., Stone, S. J., Koliwad, S., Harris, C. & Farese, R. V. Thematic review series: glycerolipids. DGAT enzymes and triacylglycerol biosynthesis. J. Lipid Res. 49, 2283–2301 (2008).

8. Shichiri, M. The role of lipid peroxidation in neurological disorders. J. Clin. Biochem. Nutr. 14–10 (2014).

9. Halliwell, B. Oxidative stress and neurodegeneration: where are we now? J. Neurochem. 97, 1634–1658 (2006).

10. Zecca, L., Youdim, M. B., Riederer, P., Connor, J. R. & Crichton, R. R. Iron, brain ageing and neurodegenerative disorders. Nat. Rev. Neurosci. 5, 863–873 (2004).

11. Tannous, B. A. Gaussia luciferase reporter assay for monitoring biological processes in culture and in vivo. Nat. Protoc. 4, 582–591 (2009).

12. Zeng, H. et al. Bi-allelic Loss of CDKN2A Initiates Melanoma Invasion via BRN2 Activation. Cancer Cell 34, 56-68.e9 (2018).

CHAPTER 3: Concluding remarks: Lipid metabolic reprograming in Glioblastoma

Over the past several decades, overall mortality rates from cancer have been declining as improvements have been made in developing targeted therapies. However, mortality in brain cancers, among which glioblastoma (GBM) is the most common and aggressive, have increased. Despite standard of care which includes tumor resection, chemotherapy, and radiation, GBM prognosis remains poor at approximately 14 months, and the 5 year survival is less than 5% [1]. Therefore, there is an urgent need for improved therapies for this disease. The investigation of therapeutic windows resulting from metabolic reprograming provides a potential therapeutic opportunity in GBM.

In many cancers, including GBM, lipid metabolic reprograming is a hallmark [2]. Broadly, alterations in lipid metabolism and composition are thought to occur in order to accommodate rapid tumor cell proliferation and facilitate survival [2]. However, there are numerous avenues by which altered lipid metabolism and composition can impact tumor cell biology. Lipids represent a unique class of metabolites with potential pro-tumorigenic effects [3]. Lipids can impact molecular signaling directly as lipid mediators [4] or indirectly by modulating membrane receptor dynamics and membrane rigidity [5]. Lipids play a critical role in maintain energy homeostasis [6] and are involved in the regulation of several cell death pathways including apoptosis and ferroptosis [7] [8].

The first evidence of altered lipid composition in GBM tumors was identified in the 1960's with gas–liquid chromatography of tumors and normal brain samples [9] where the levels of polyunsaturated fatty acids, particularly linoleic acids, were observed to be higher in gliomas, meningiomas and neurinomas than in the normal brain. More recent studies have corroborated these results and pointed to specific lipid classes enriched in GBM tumors, specifically

triacylglycerides and cholesterol esters [10]. As a functional validation of these lipidomic observations, lipid droplets – organelles largely composed of neutral lipids such as cholesterol esters and triacylglycerides - have been shown to be enriched in GBM tumors compared to the normal brain [11]. Technological improvements have enabled increasingly greater resolution of lipid compositional alterations in tumors over the decades. Studies investigating altered lipid composition in GBM have continued to present day and further shed increasing resolution of these lipid composition changes.

The critical gap in knowledge is to understand how these lipid compositional changes occur. In many cancers, transcriptional and genomic alterations induce aberrant lipid metabolism to support critical cell functions and promote tumour growth [12]. These alterations, including those in p53, EGFR, MDM2/4, and PTEN, frequently occur in GBM. Glioblastoma displays intertumoral molecular heterogeneity, with frequent somatic alterations in signal transduction and tumour suppressor pathways [13]. However, the full array of molecular alterations underlying aberrant lipid metabolism in GBM, and their consequences on tumour cell biology are not well understood.

It is also becoming increasing clear that cancer cell metabolism is impacted by the tumour microenvironment (TME) [14] and extrinsic factors can drive metabolic reprograming in cancer [15]. Cancers with metabolic flexibility can adapt to nutrient and oxygen-depleted environments by upregulating fatty acid oxidation or biosynthesis. Tumor cells interact with normal brain cells to exchange nutrients, secreted factors, and neurotransmitters to promote GBM growth [16]. Importantly, in vitro systems supply only limited essential fatty acids, increasing the need for lipid

biosynthesis and resulting in culture artifacts. A relevant example of environment-dependent lipid metabolic dependencies is the connection between cholesterol biosynthesis and scavenging. It has been shown that in cholesterol-free in vitro environments, GBM cells require cholesterol biosynthesis for survival [17]. However, blocking cholesterol biosynthesis in GBM cells has no effect when extracellular cholesterol is available for scavenging [18]. Studying GBM within a cholesterol-free in vitro system might allow one to draw the erroneous conclusion that inhibiting cholesterol biosynthesis with a statin, for example, would be an effective therapeutic option in GBM. The physiologic context that includes extracellular lipids, which are available in the brain tumor microenvironment, revealed that indeed inhibitors for both scavenging and biosynthesis would be required. Therefore, in vivo systems and direct-from-patient samples are necessary to study the GBM lipidome under physiologic conditions of lipid and nutrient scavenging and TME-dependent interactions.

In chapter 1 of this work, we describe the many molecular mechanisms by which tumor metabolism may be altered by both oncogenic events as well as the tumor microenvironment. Critical for the study of GBM, the brain itself is a unique microenvironment which is tightly regulated and unique from many other organs in the body [19]. Future studies of GBM will need to consider the many physical factors of the brain tumor microenvironment and account for those specific factors in order to reveal true biology and not experimental artifacts.

In chapter 2 of this work, we perform a comprehensive characterization of the GBM lipidome across molecularly heterogenous patient tumors and diverse tumor microenvironments. Firstly, we observed similar enrichments of cholesterol esters and triacylglycerides in tumor compared to

normal brain tissues as observed previously. Most importantly, however, we identified that the GBM lipidome itself is heterogeneous across unique patient tumors. This work truly explores the heterogeneity of the GBM lipidome between a large cohort (n=114) of GBM patient tumors with a breadth of scope and depth of analysis that had not been achieved previously. Importantly, the investigation of the GBM lipidome across diverse tumor microenvironments in patient tumors, orthotopic xenografts, and gliomaspheres allowed for the identification of biologically relevant signatures. Critically, it was the pairing of lipidomic, genomic, and transcriptomic datasets together which allowed for the novel observation of CDKN2A as a regulator of the GBM lipidome. Importantly, we connected this unique lipidome with a metabolic vulnerability related to lipid peroxidation and ferroptosis. The work described in chapter 2 is most likely just the beginning of the interpretation of this comprehensive characterization. Future studies will aim to identify additional molecular features and their associations with the GBM lipidome, to continue to shed light on the dynamic and evolving field of lipid metabolism.

REFERENCES

1. Glioblastoma Multiforme: A Review of its Epidemiology and Pathogenesis through Clinical Presentation and Treatment.
2. Snaebjornsson, M. T., Janaki-Raman, S. & Schulze, A. Greasing the wheels of the cancer machine: the role of lipid metabolism in cancer. *Cell Metab.* **31**, 62–76 (2020).
3. Pavlova, N. N. & Thompson, C. B. The emerging hallmarks of cancer metabolism. *Cell Metab.* **23**, 27–47 (2016).
4. Sulciner, M. L., Gartung, A., Gilligan, M. M., Serhan, C. N. & Panigrahy, D. Targeting lipid mediators in cancer biology. *Cancer Metastasis Rev.* **37**, 557–572 (2018).
5. Swinnen, J. V., Dehairs, J. & Talebi, A. Membrane lipid remodeling takes center stage in growth factor receptor-driven cancer development. *Cell Metab.* **30**, 407–408 (2019).
6. Koundouros, N. & Poulogiannis, G. Reprogramming of fatty acid metabolism in cancer. *Br. J. Cancer* **122**, 4–22 (2020).
7. Dixon, S. J. & Stockwell, B. R. The hallmarks of ferroptosis. *Annu. Rev. Cancer Biol.* **3**, 35–54 (2019).
8. Chen, X., Kang, R., Kroemer, G. & Tang, D. Broadening horizons: the role of ferroptosis in cancer. *Nat. Rev. Clin. Oncol.* **18**, 280–296 (2021).
9. GOPAL, K., GROSSI, E., PAOLETTI, P. & USARDI, M. LIPID COMPOSITION OF HUMAN INTRACRANIAL TUMORS: A BIOCHEMICAL STUDY. *Acta Neurochir. (Wien)* **11**, 333–347 (1963).
10. Tosi, M. R. & Tugnoli, V. Cholesteryl esters in malignancy. *Clin. Chim. Acta Int. J. Clin. Chem.* **359**, 27–45 (2005).

11. Geng, F. & Guo, D. Lipid droplets, potential biomarker and metabolic target in glioblastoma. *Intern. Med. Rev. Wash. DC Online* **3**, (2017).

12. Guo, D., Bell, E. H. & Chakravarti, A. Lipid metabolism emerges as a promising target for malignant glioma therapy. *CNS Oncol.* **2**, 289–299 (2013).

13. Brennan, C. W. *et al.* The somatic genomic landscape of glioblastoma. *Cell* **155**, 462–477 (2013).

14. Dey, P., Kimmelman, A. C. & DePinho, R. A. Metabolic codependencies in the tumor microenvironment. *Cancer Discov.* **11**, 1067–1081 (2021).

15. Muir, A., Danai, L. V. & Vander Heiden, M. G. Microenvironmental regulation of cancer cell metabolism: implications for experimental design and translational studies. *Dis. Model. Mech.* **11**, dmm035758 (2018).

16. Gillespie, S. & Monje, M. The neural regulation of cancer. *Annu. Rev. Cancer Biol.* **4**, 371–390 (2020).

17. Ahmad, F., Sun, Q., Patel, D. & Stommel, J. M. Cholesterol Metabolism: A Potential Therapeutic Target in Glioblastoma. *Cancers* **11**, (2019).

18. Guo, D. *et al.* An LXR agonist promotes glioblastoma cell death through inhibition of an EGFR/AKT/SREBP-1/LDLR-dependent pathway. *Cancer Discov.* **1**, 442–456 (2011).

19. Quail, D. F. & Joyce, J. A. The Microenvironmental Landscape of Brain Tumors. *Cancer Cell* **31**, 326–341 (2017).